Received June 10, 2014, accepted July 9, 2014, date of publication July 16, 2014, date of current version August 8, 2014.

Digital Object Identifier 10.1109/ACCESS.2014.2340874

Signals of Interest Recovery With Multiple Receivers Using Reference-Based Successive Interference Cancellation for Signal Collection Applications

RIC A. ROMERO, ALEXANDER RIOS, AND TRI T. HA

Corresponding author: R. A. Romero (rnromero@nps.edu)

Naval Postgraduate School, Monterey, CA 93943, USA

ABSTRACT In this paper, we introduce a novel but intuitive scheme to recover multiple signals of interest (SoI) from multiple emitters in signal collection applications such as signal intelligence, electronic intelligence, and communications intelligence. We consider a case where the SoIs form a heavy interference environment. The scheme, which is referred to as reference-based successive interference cancellation (RSIC), involves a combination of strategic receiver placement and signal processing techniques. The scheme works by placing a network of cooperative receivers where each receiver catches its own SoI (despite multiple interferences). The first receiver demodulates the initial SoI (called a reference signal) and forwards it to the second receiver. The second receiver collects a received signal containing the second SoI but is interfered with by the initial SoI, which is a problem called co-channel interference in cellular communications. Unfortunately, the amplitude scaling of the interference is unknown in the second receiver and therefore has to be estimated via least squares error. It turns out that the estimation requires *a priori* knowledge of the second SoI, which is the very signal it tries to demodulate, thereby yielding a Catch-22 problem. We propose using an initial guess on the second SoI to form an amplitude estimate such that the interference is subtracted (cancelled) from the collected measurement at the second receiver. The procedure is applied to a third receiver (or multiple receivers) until the last of the desired SoI is separated from all of the co-channel interferences. The RSIC scheme performs well. Using quaternary phase shift keying as example modulation, we present major symbol error rate (SER) performance improvements with the use of RSIC over the highly degraded SER of receivers that are heavily interfered and do not employ any cancellation technique.

INDEX TERMS Amplitude estimation, COMINT, ELINT, LSE, QPSK, signal collection, RSIC, SIGINT, SoI.

I. INTRODUCTION

Wireless signals from various emitters such as cellular communications, commercial/military radar, non-intentional interferences and even intentional interferences (such as jammers and cyber attacks) are now commonplace. Our interest is in the collection of some these signals which we refer to as signal/s of interest (SoI). Examples of signal collection applications are signal intelligence (SIGINT) [1], electronic intelligence (ELINT) [2], and communications intelligence (COMINT) [3] applications. Works in these collection-related fields in the open literature are few and far between. However, we refer [1], [4], and [5] as starting points for the uninitiated when it comes to SIGINT. We refer the interested reader to [2] as an excellent text for ELINT. The works in [6]–[8] relate ELINT to radar. For potential COMINT application, [9] and [10] present good exposure to communication modulation classification and contain other references related to that area.

Unlike a single-receiver system that tries to collect and retrieve multiple signals, this work uses multiple receivers to collect multiple signals. We introduce a method that allows subtraction of heavy interferences from a received signal by a particular receiver so that the desired signal is ''faithfully'' reconstructed (i.e. demodulated signals for communications

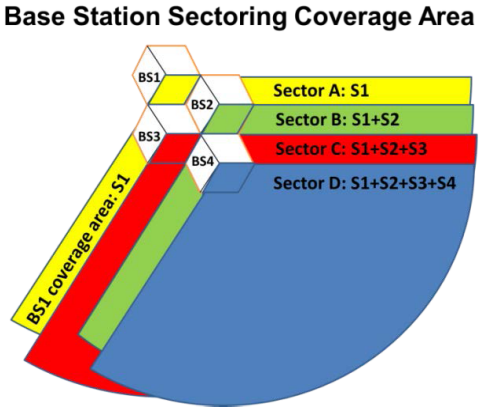

FIGURE 1. A 4-cell BS configuration with overlapping antenna coverage which has different signal combinations received in each sector. The co-channel signals are generically labeled S1, S2, S3, and S4.

and radar applications). To demodulate different SoIs from different emitters, multiple receivers are positioned so that an initial reference signal is collected that is passed on to the second receiver that effectively conducts a variation on co-channel interference (CCI) cancellation. Our interest is in the use of multiple receivers that are physically far apart in contrast to one-receiver collector or multi-antenna collector (co-located receivers) which uses classical successive interference cancellation (SIC) techniques geared towards demodulating one signal (or more) from many (e.g. co-channel interference) where [11] and [12] are good starting articles and contain many references for readers that are interested in that topic. In this paper, we are not interested in these types of SIC techniques for a one-receiver or multi-antenna collector. Again, our interest is in the use of multiple receiver collectors that are strategically positioned to cooperate so that each one receiver demodulates its own signal of interest (SoI) [13] from various transmitters thereby yielding multiple SoIs for signal collection purposes. In this scenario where potentially many receivers are involved, latency and error accumulation are expected in the demodulation of the latter SoIs. For applications conducting long-term surveillance and collection, latency is acceptable and in fact is expected. Thus, the technique of using multiple receivers for successive cancellation (or more aptly successive subtraction) applies very appropriately.

We call our method reference-based successive interference cancellation (RSIC) technique. This method is novel in the sense that most signal collection applications use one large super sensitive receiver while RSIC employs multiple receivers (but not necessarily highly sensitive) that are spatially far apart. RSIC is very intuitive and elegantly simple but

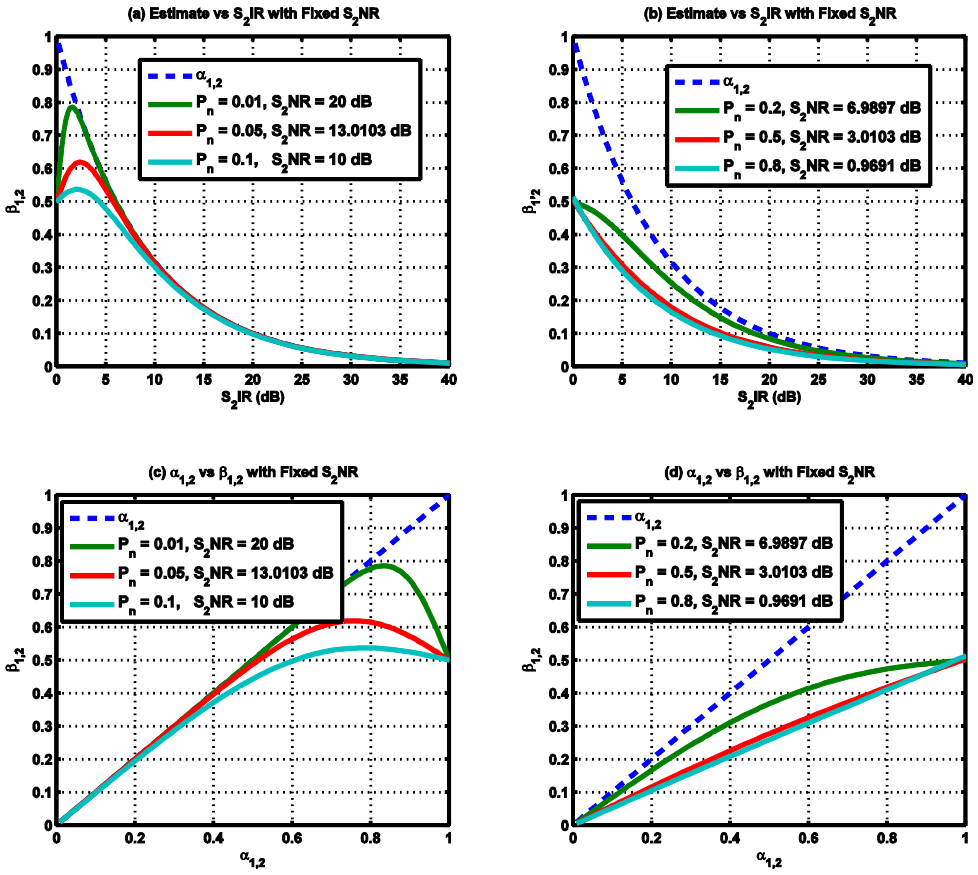

FIGURE 2. The estimation curves as function of S_2IR at various S_2NR: (a) estimate with high S_2NR; (b) estimate with low S_2NR; (c) $\beta_{1,2}$ vs. $\alpha_{1,2}$ with high S_2NR; and (d) $\beta_{1,2}$ vs. $\alpha_{1,2}$ with low S_2NR.

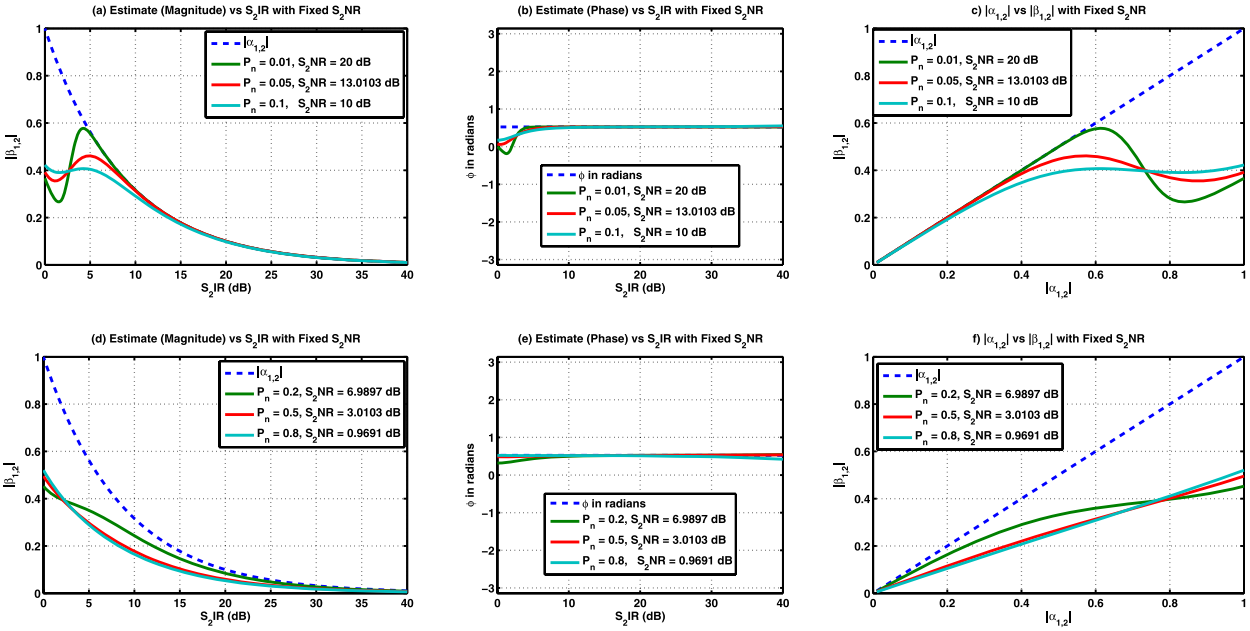

FIGURE 3. The estimation curves as function of S_2IR at various S_2NR where the amplitude phase offset is $\pi/6$ or 30 deg: (a) estimate (magnitude) with high S_2NR; (b) estimate (phase) with high S_2NR; (c) $|\beta_{1,2}|$ vs. $|\alpha_{1,2}|$ with high S_2NR; (d) estimate (magnitude) with low S_2NR; (e) estimate (phase) with low S_2NR; and (f) $|\beta_{1,2}|$ vs. $|\alpha_{1,2}|$ with low S_2NR.

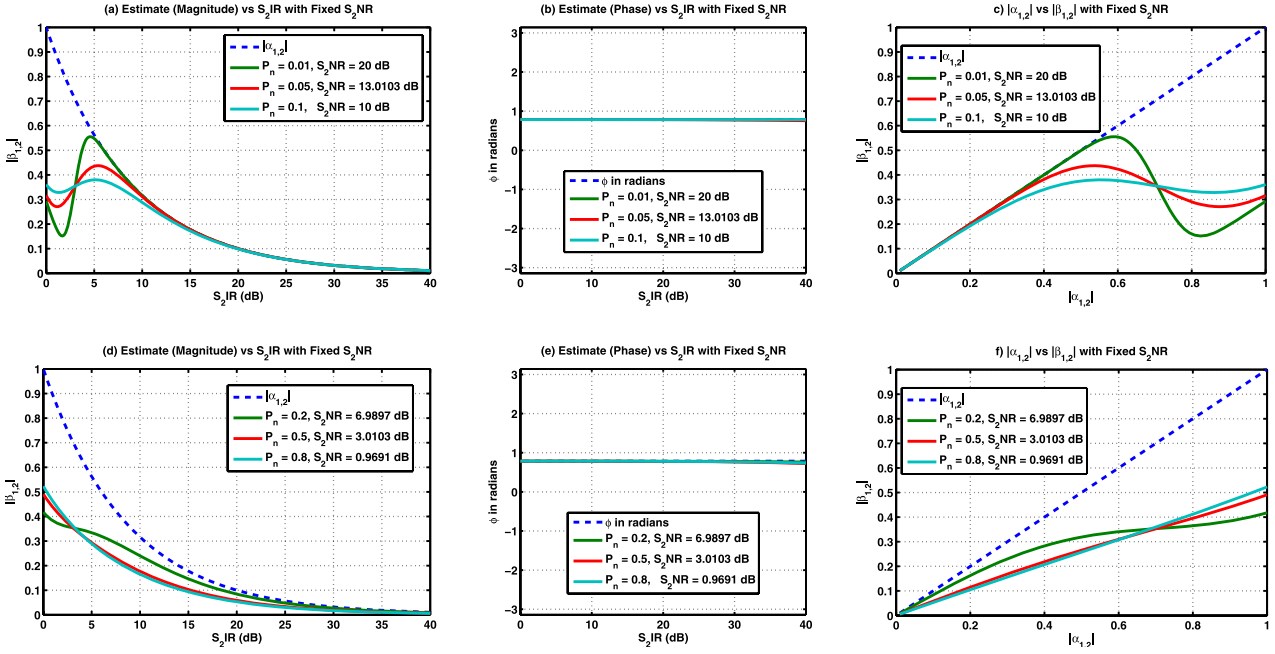

FIGURE 4. The estimation curves as function of S_2IR at various S_2NR: (a) estimate (magnitude) with high S_2NR is $\pi/4$ or 45 deg; (b) estimate (phase) with high S_2NR; (c) $|\beta_{1,2}|$ vs. $|\alpha_{1,2}|$ with high S_2NR; (d) estimate (magnitude) with low S_2NR; (e) estimate (phase) with low S_2NR; and (f) $|\beta_{1,2}|$ vs. $|\alpha_{1,2}|$ with low S_2NR.

it will be evident quickly that the application problem it solves presents very difficult and unique challenges. RSIC works by strategically placing an initial receiver in a favorable location (i.e. not heavily interfered but not noise-free) where an initial SoI is readily collected and demodulated. This reference signal is then transmitted to a second receiver (and others for multi-receiver scenario). The second receiver is placed where its corresponding SoI is corrupted by the first receiver's SoI. Unfortunately, the reference signal cannot simply be cancelled or subtracted from the second receiver received signal. This is because the power (i.e. the amplitude or gain) of the first SoI may not be known in the second receiver (which is a very practical assumption especially in signal collection application). In this work, we attempt to estimate the amplitude (complex or real) of the interference despite the fact the second SoI becomes an "interferer" to first

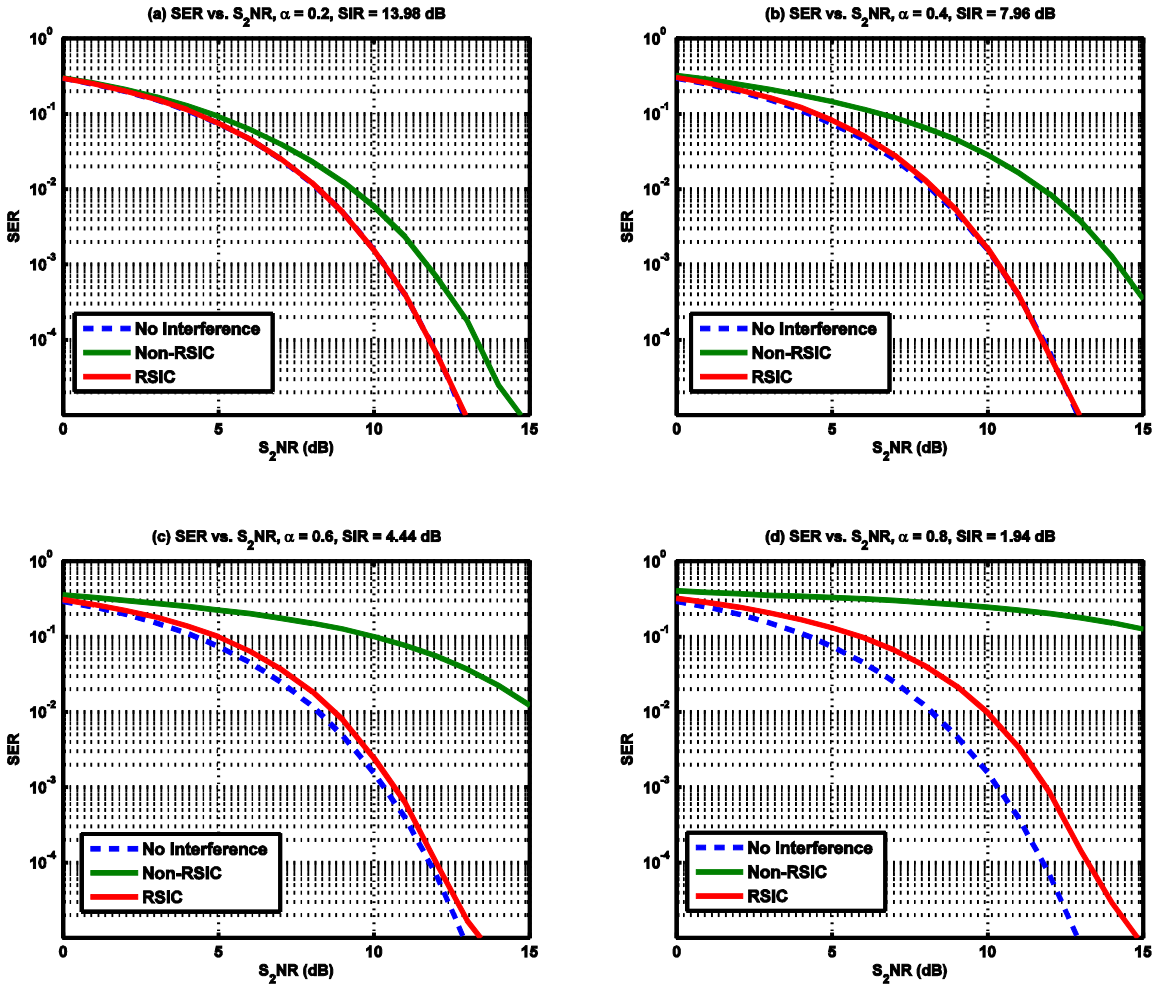

FIGURE 5. The SER vs. S_2NR (s_2 demodulation) performance curves for MLD receiver with no interference (interference-free), Non-RSIC (MLD with interference), and RSIC for various interference powers: (a) $\alpha_{1,2} = 0.2$, $S_2IR = 14$ dB; (b) $\alpha_{1,2} = 0.4$, $S_2IR = 7.96$ dB; (c) $\alpha_{1,2} = 0.6$, $S_2IR = 4.44$ dB; (d) $\alpha_{1,2} = 0.8$, $S_2IR = 1.94$ dB.

SoI in terms of estimation. This is an interesting twist. Recall that from the second receiver's demodulation standpoint, it is the first SoI that is the actual interference. Moreover, the estimation needs actual knowledge of the second SoI, the very signal it tries to demodulate yielding a "Catch-22" problem! Assuming we are able to overcome this problem and thus are able to calculate an estimate for the SoI amplitude, we can then scale the reference with that estimate. Before demodulation, the scaled reference is subtracted from the second receiver's received signal. The result is then demodulated as second SoI. Now a "cleaned up" version of the second signal is available and is made into a second reference signal, which is passed on to a third receiver (and others in the system). The cancellation procedure is repeated until a cleaner reference is available to a fourth receiver. Thus, the procedure applies to multiple receivers.

In this work, we present a mathematical model with several receivers with multiple interferers. We attempt to estimate the amplitudes of the received interfering signals to be used for cancellation. We evaluate the performance of the RSIC technique both in terms of symbol error rates (SER) and parameter estimation. The technique presented here works for various scenarios where the signals can be of various types and modulation. For presentation of results, we consider an example scenario where we collect communication signals using QPSK modulation. To successfully estimate these interference amplitudes, we use least squares error (LSE) estimation method. LSE is a mature estimation technique and thus references abound but we point the novice reader to an excellent text [14]. Utilizing Monte Carlo simulation, we calculate SER against various signal-to-noise ratios (SNR), signal-to-interference (SIR), and signal-to-interference plus noise combinations.

The major contribution of this paper is the introduction of a novel and yet intuitive technique (RSIC) that solves the multiple-signal recovery problem (from many emitters and thus heavy interference) by the combination of strategic placement of multiple receivers and a clever mix of signal processing techniques. This involves solving

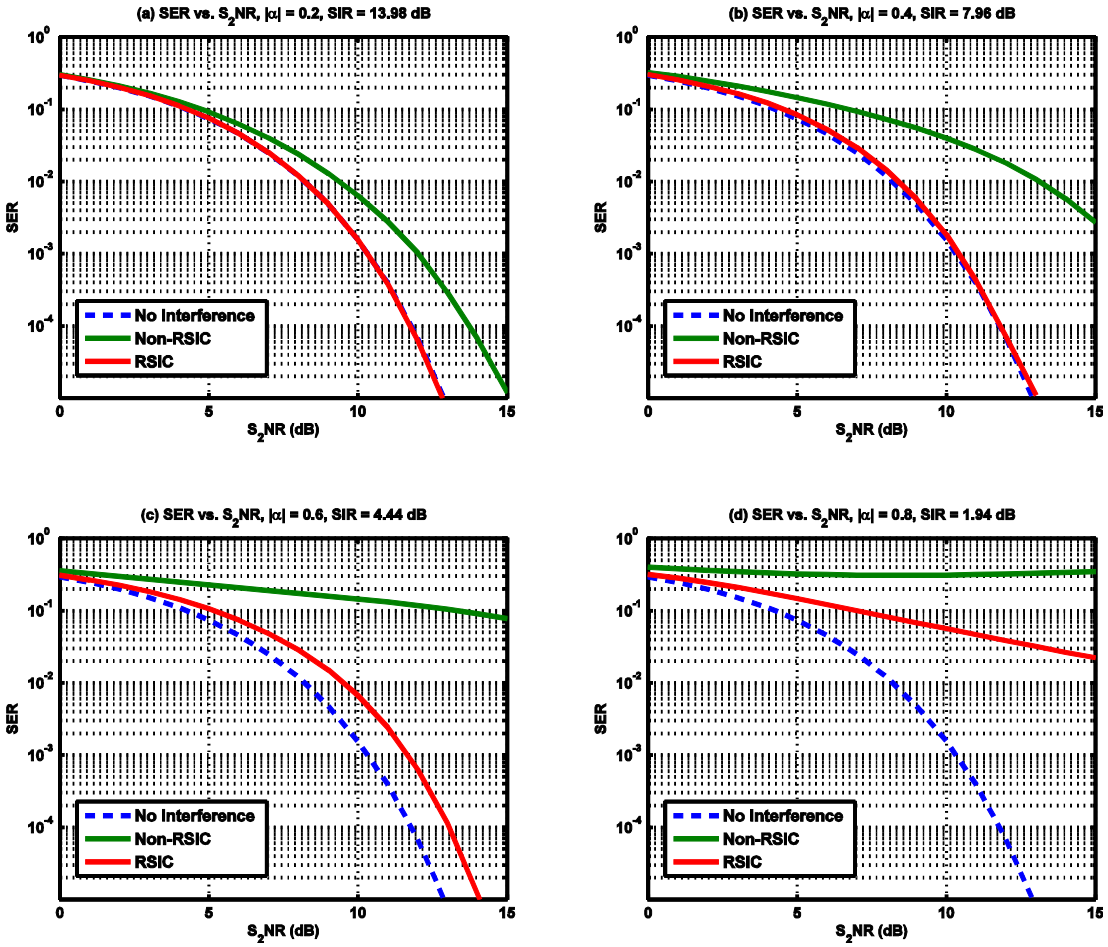

FIGURE 6. The SER vs. S_2NR (with $\phi = \pi/6$) performance curves for MLD receiver with no interference (interference-free), Non-RSIC (MLD with interference), and RSIC for various interference powers: (a) $|\alpha_{1,2}| = 0.2$, $S_2IR = 14$ dB; (b) $|\alpha_{1,2}| = 0.4$, $S_2IR = 7.96$ dB; (c) $|\alpha_{1,2}| = 0.6$, $S_2IR = 4.44$ dB; (d) $|\alpha_{1,2}| = 0.8$, $S_2IR = 1.94$ dB.

the need to have knowledge of the signal being demodulated, amplitude estimation, and successive cancellation. In the example scenario of collecting QPSK signals from multiple emitters (e.g. base stations), major receiver performance improvements in terms of SoI SERs as well as parameter estimation for individual receivers are shown. The paper is organized as follows. In Section II, the concept of how to strategically place receivers in relation to emitter configuration is discussed. The signal mathematical models needed for the RSIC technique are discussed in detail. LSE of complex-valued amplitude estimators is presented. The inherent but interesting problem of needing a priori knowledge of the signal to be demodulated to accomplish estimation is addressed. In Section III, IV, and V, SER and estimation results for a two-receiver system, a three-receiver system and a four-receiver system using QPSK modulation are presented respectively. In relation to SER, we observe how the estimates change as a function of SNR and different interference amplitude combinations (i.e. various SIR combinations). In Section VI, we present our conclusions.

II. REFERENCE-BASED SUCCESSIVE INTERFERENCE CANCELLATION

The set of emitters that transmit multiple SoIs may exist in many configurations and is therefore application dependent. For illustrative purposes, let us assume that the emitters are base station (BS) transmitters and as such transmit cellular signals. A good example of a 4-cell BS configuration is shown in Fig. 1, where the antenna or coverage areas of multiple cellular base stations (BSs) overlap with those from subsequent BSs. This configuration results in a layout where different regions contain multiple co-channel signals. Certain sectors of the coverage areas contain only a specific number of these signals and one area contains only one signal. It turns out that any cellular configuration features a specific area where only one signal is contained (and therefore RSIC can be applied to any configuration).

For $1, 2, \ldots, L$ coverage areas, each sector is modeled so that it contains a received signal vector that is described by

$$\mathbf{y}_n = \mathbf{s}_n + \sum_{m=1}^{n-1} \alpha_{m,n}\mathbf{s}_m + \mathbf{w}_n \tag{1}$$

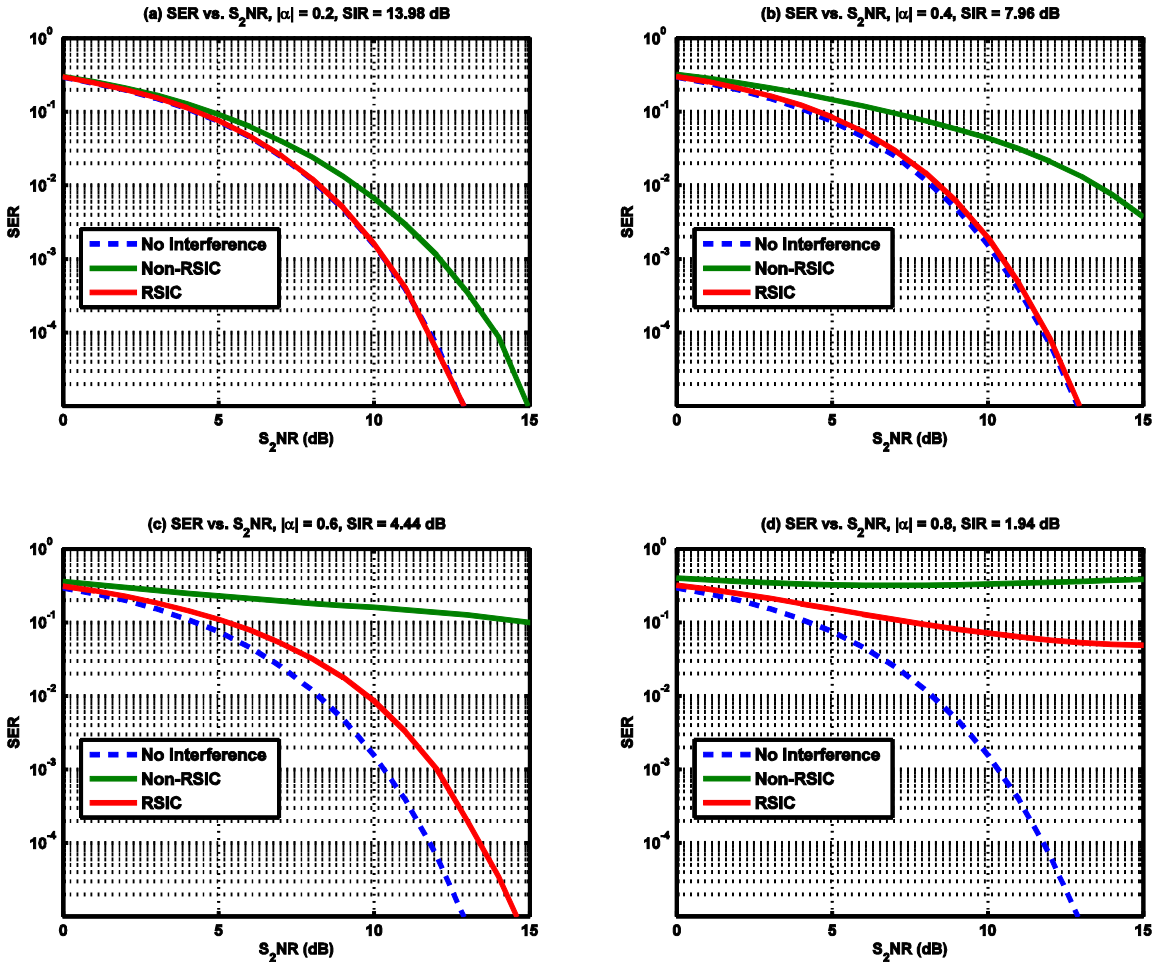

FIGURE 7. The SER vs. S_2NR (with $\phi = \pi/4$) performance curves for MLD receiver with no interference (interference-free), Non-RSIC (MLD with interference), and RSIC for various interference powers: (a) $|\alpha_{1,2}| = 0.2$, $S_2IR = 14$ dB; (b) $|\alpha_{1,2}| = 0.4$, $S_2IR = 7.96$ dB; (c) $|\alpha_{1,2}| = 0.6$, $S_2IR = 4.44$ dB; (d) $|\alpha_{1,2}| = 0.8$, $S_2IR = 1.94$ dB.

where n serves as index for the n^{th} receiver (Rx_n), $\mathbf{s}_n$ is the signal corresponding to base station n (BS_n), and w_n is the complex-valued additive white Gaussian noise (AWGN) in Rx_n. A signal vector $\mathbf{s}_m$ corresponds to base station m (BS_m) and $\alpha_{m,n}$ is its amplitude gain (or loss). In other words, for Rx_n the SoI is $\mathbf{s}_n$ and the $n-1$ vectors described by $\mathbf{s}_m$ serve as interfering signals (known as CCI in cellular applications) in Rx_n. The amplitude $\alpha_{m,n}$ may take on various values and dictate the SIR. The amplitude $\alpha_{m,n}$ can be real (and positive) as in synchronous systems. In general, $\alpha_{m,n}$ is complex-valued to account for the fact that the signal symbols received by the current receiver in (1) from multiple transmitters may not be aligned in time. In other words, the symbols are not phased-synchronized in the receiver. If $\alpha_{m,n}$ is real and positive, then the signal symbols are received synchronously. If $\alpha_{m,n}$ is complex, then its phase (and magnitude) may be estimated.

Let the amplitude estimate for $\alpha_{m,n}$ be $\beta_{m,n}$. If the estimates $\beta_{m,n}$ are readily available, then it is straightforward to perform the interference subtraction or cancellation via

$$\check{\mathbf{s}}_n = \mathbf{y}_n - \sum_{m=1}^{n-1} \beta_{m,n}\mathbf{s}_m \tag{2}$$

where $\check{\mathbf{s}}_n$ serves as the pre-demodulation signal. Thus, demodulation in the n^{th} receiver is given by

$$\hat{\mathbf{s}}_n = \text{dec}(\check{\mathbf{s}}_n) \tag{3}$$

where dec(*) stands for receiver decision via the standard maximum-likelihood detection (MLD). For high SNR, the noise is considered negligible and thus the receiver becomes interference-limited. For low SNR, the receiver becomes noise-limited and therefore the noise may even have a greater effect on receiver performance than the interferences themselves.

A. INTERFERENCE AMPLITUDE ESTIMATION WITH LSE

Starting with the notion of a L-receiver system with index n in (1), we propose to utilize LSE to determine estimates for the $\alpha_{m,n}$ values. In this paper we assume vector signal models. This is appropriate since signals in modern receivers are

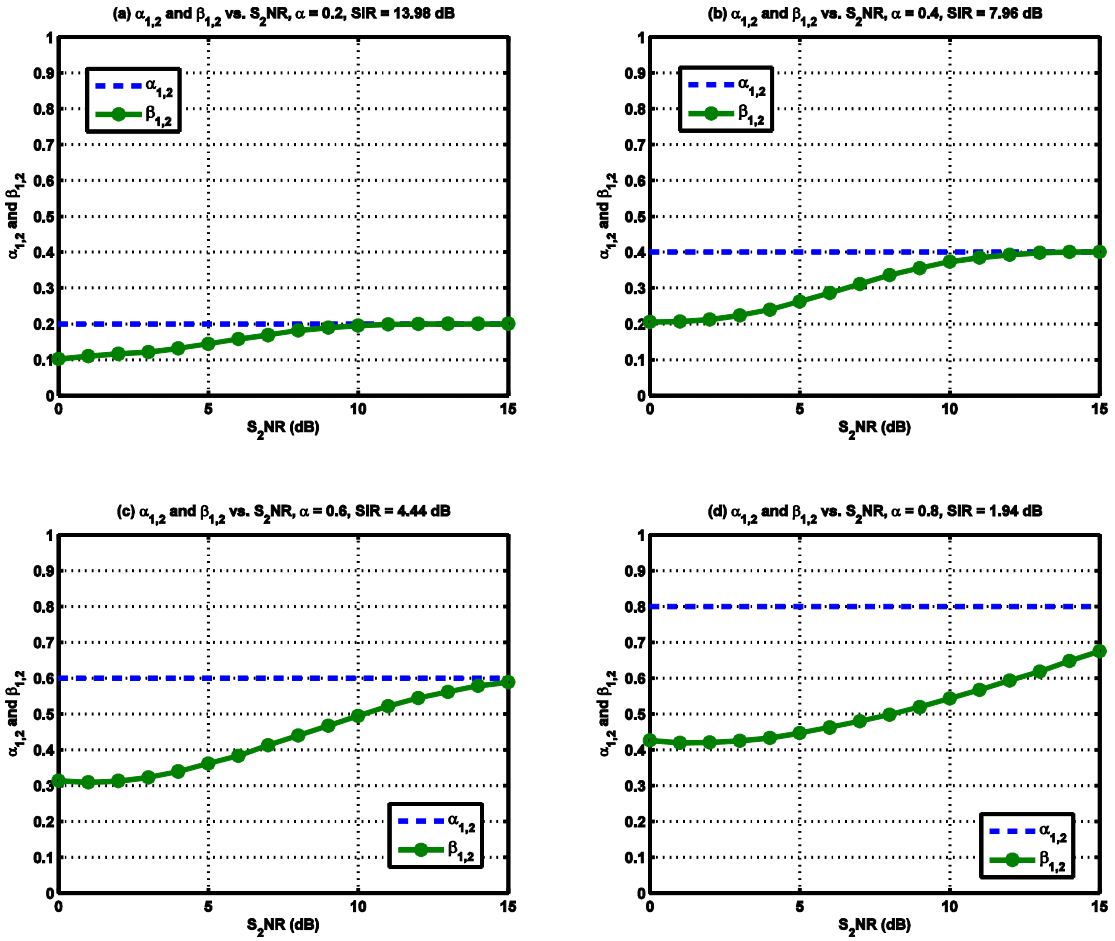

FIGURE 8. The estimate plots of $\alpha_{1,2}$ and the estimator $\beta_{1,2}$ vs. S_2NR values for: (a) $\alpha_{1,2} = 0.2$, S_2IR = 14 dB, (b) $\alpha_{1,2} = 0.4$, S_2IR = 7.96 dB; (c) $\alpha_{1,2} = 0.6$, S_2IR = 4.44 dB, and (d) $\alpha_{1,2} = 0.8$, S_2IR = 1.94 dB.

almost always sampled prior to signal processing. We determine the estimates of complex amplitudes by first minimizing the squared magnitude difference between the received signal $\mathrm{y}_n = [\mathrm{y}_n[0]\mathrm{y}_n[1]\cdots\mathrm{y}_n[N-1]]^T$ in Rx_n and the sum signal $\mathbf{s}_n + \sum_{m=1}^{n-1} \alpha_{m,n}\mathbf{s}_m$ where the m^{th} interfering signal is given by $\mathbf{s}_m = [s_m[0]\ s_m[1]\cdots s_m[N-1]]^T$ and $\mathbf{s}_n$ is the actual SoI. The error is given by

$$J(\boldsymbol{\alpha}_n) = \sum_{i=0}^{N-1} \left| y_n[i] - (s_n[i] + \sum_{m=1}^{n-1} \alpha_{m,n} s_m[i]) \right|^2 \tag{4}$$

where $J(\boldsymbol{\alpha}_n)$ is the square-error magnitude, N is the number of samples (or symbols) in the measurement with i being the index, and $\boldsymbol{\alpha}_n = [\alpha_{1,n}\ \alpha_{2,n}\cdots\alpha_{n-1,n}]^T$ is the interference amplitude vector whose components are $\alpha_{m,n}$. As such (4) is equivalent to

$$\begin{aligned} J(\boldsymbol{\alpha}_n) &= \left\| \mathbf{y}_n - \left(\mathbf{s}_n + \sum_{m=1}^{n-1} \alpha_{m,n}\mathbf{s}_m \right) \right\|^2 \\ &= \left(\mathbf{y}_n - \mathbf{s}_n - \sum_{m=1}^{n-1} \alpha_{m,n}\mathbf{s}_m \right)^H \left(\mathbf{y}_n - \mathbf{s}_n - \sum_{m=1}^{n-1} \alpha_{m,n}\mathbf{s}_m \right) \\ &= \left(\mathbf{y}_n - \mathbf{s}_n - \mathbf{S}\boldsymbol{\alpha}_n \right)^H \left(\mathbf{y}_n - \mathbf{s}_n - \mathbf{S}\boldsymbol{\alpha}_n \right) \end{aligned} \tag{5}$$

where $(\cdot)^H$ is the Hermitian or complex conjugate transpose operation, and $\mathbf{S} = [\mathbf{s}_1\ \mathbf{s}_2\cdots\mathbf{s}_{n-1}]$ is an $N \times (n-1)$ interference signal matrix (ISM) where $N \geq (n-1)$. Since our application is signal collection (where large or big data collection is typical) we assume that $N \gg (n-1)$. Taking the partial derivative of (5) with respect to $\boldsymbol{\alpha}_n$ yields the $(n-1) \times 1$ column vector (see Appendix for complete derivation) given by

$$\frac{\partial J(\boldsymbol{\alpha}_n)}{\partial \boldsymbol{\alpha}_n} = -\left[\mathbf{S}^H \left(\mathbf{y}_n - \mathbf{s}_n \right) \right]^* + \left[\mathbf{S}^H \mathbf{S}\boldsymbol{\alpha}_n \right]^*. \tag{6}$$

Letting the derivative vector be equal to zero vector yields

$$\mathbf{S}^H \mathbf{S}\boldsymbol{\alpha}_n = \mathbf{S}^H \left(\mathbf{y}_n - \mathbf{s}_n \right). \tag{7}$$

Then the estimate $\boldsymbol{\beta}_n$ of the amplitude vector $\boldsymbol{\alpha}_n$ is calculated to be

$$\boldsymbol{\beta}_n = (\mathbf{S}^H\mathbf{S})^{-1}\mathbf{S}^H \left(\mathbf{y}_n - \mathbf{s}_n \right). \tag{8}$$

If the elements of amplitude gain vector $\boldsymbol{\alpha}_n$ are real then it can be shown that (see Appendix for complete derivation) that the

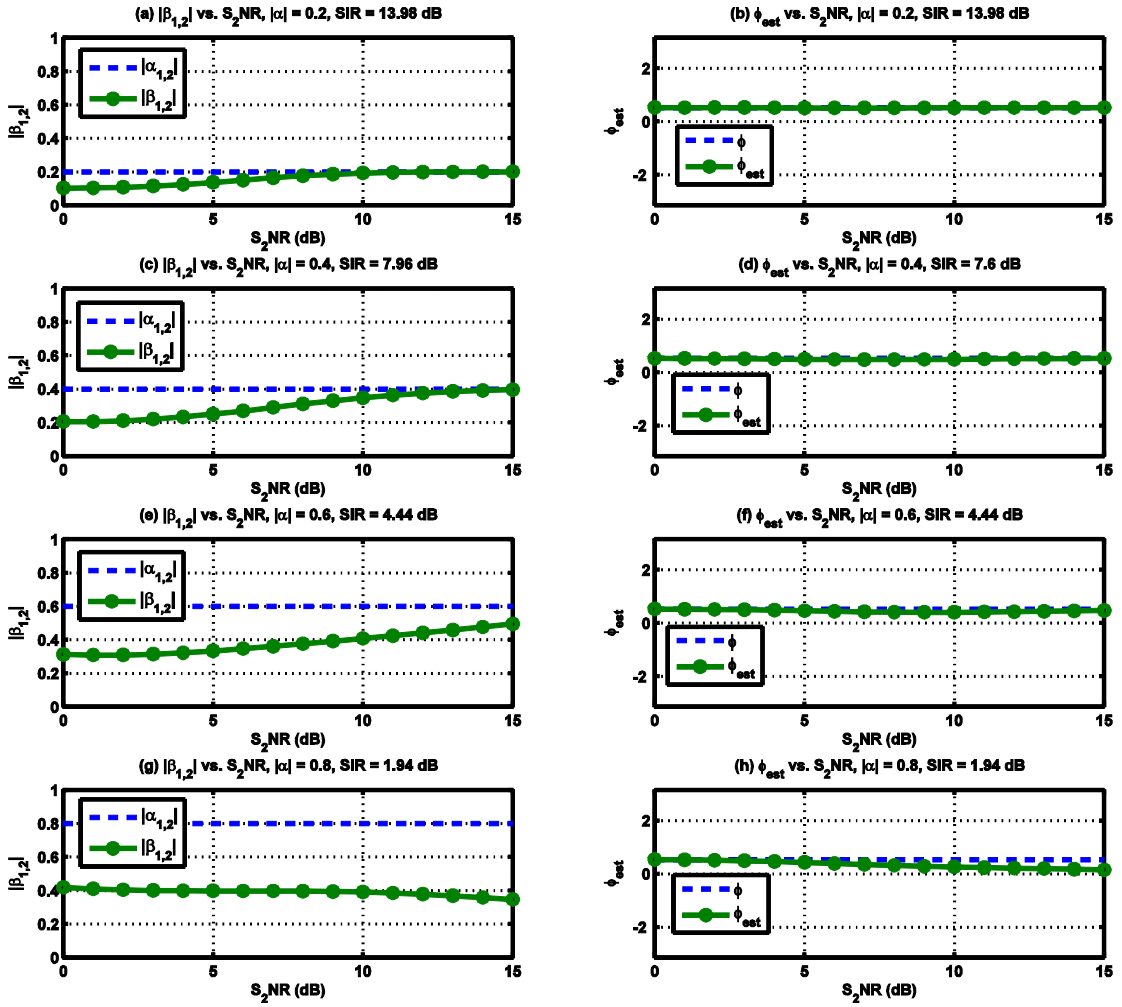

FIGURE 9. Magnitude and phase estimates ($\beta_{1,2}$) vs. S_2NR values for $\alpha_{1,2}$ with $\phi = \pi/6$: (a) magnitude and (b) phase for $|\alpha_{1,2}| = 0.2$; (c) magnitude and (d) phase for $|\alpha_{1,2}| = 0.4$; (e) magnitude and (f) phase for $|\alpha_{1,2}| = 0.6$; and (g) magnitude and (h) phase for $|\alpha_{1,2}| = 0.8$.

amplitude vector estimate is given by

$$\boldsymbol{\beta}_n = [\mathrm{Re}(\mathbf{S}^H\mathbf{S})]^{-1}\mathrm{Re}[\mathbf{S}^H(\mathbf{y}_n - \mathbf{s}_n)]. \quad (9)$$

The equations (8) and/or (9) form the starting point of the RSIC method in terms of estimating the amplitude vector needed to be applied to the reference signals such that the subtraction of the multiple interference signals from the received signal in any receiver in the receiver chain may be performed. Unfortunately, in (8) we already see two major issues. The first is that (8) assumes that the true ISM $\mathbf{S} = [\mathbf{s}_1\ \mathbf{s}_2\ \cdots\ \mathbf{s}_{n-1}]$ is known a priori. Second, (8) also assumes that $\mathbf{s}_n$ is available. If that were the case then there's no need to subtract interferers since the SoI $\mathbf{s}_n$ is already available (which we know is not true since $\mathbf{s}_n$ is the very signal that Rx_n is trying to capture and demodulate).

B. REFERENCE SIGNALS VIA STRATEGIC RECEIVER PLACEMENT

Since the receivers do not have prior knowledge of the interfering signals (the ISM given by $\mathbf{S} = [\mathbf{s}_1\ \mathbf{s}_2\ \cdots\ \mathbf{s}_{n-1}]$), we have to devise a way for these receivers to gain some knowledge of these SoIs. We do so by strategic placement of the receivers. The starting point is with an initial receiver collecting lightly interfered or interference-free SoI. Of course, the first SoI is not noise-free because of its own receiver noise. In Fig. 1, this is implemented with Rx_1 located in Sector A receiving $\mathbf{s}_1$. Rx_1 takes the first SoI and demodulates it (using MLD) as "first reference" $\hat{\mathbf{s}}_1$, and transmits this reference to Rx_2 (and other receivers for multi-receiver scenario) located in Sector B. This can easily be performed using another channel (away from the SoI channels). Recall that our application is signal collection, i.e. the Rxs are not necessarily mobile or cellular phones. In other words, these collector receivers are pre-configured such that they use separate means (e.g. separate channels) for accomplishing the transmission of reference signals. In our Monte Carlo experiments, we assume that these references are received with sufficient or high SNR. The topic of "separate channels" is also interesting since it touches on the cooperative networking aspect of the implementation but is beyond the

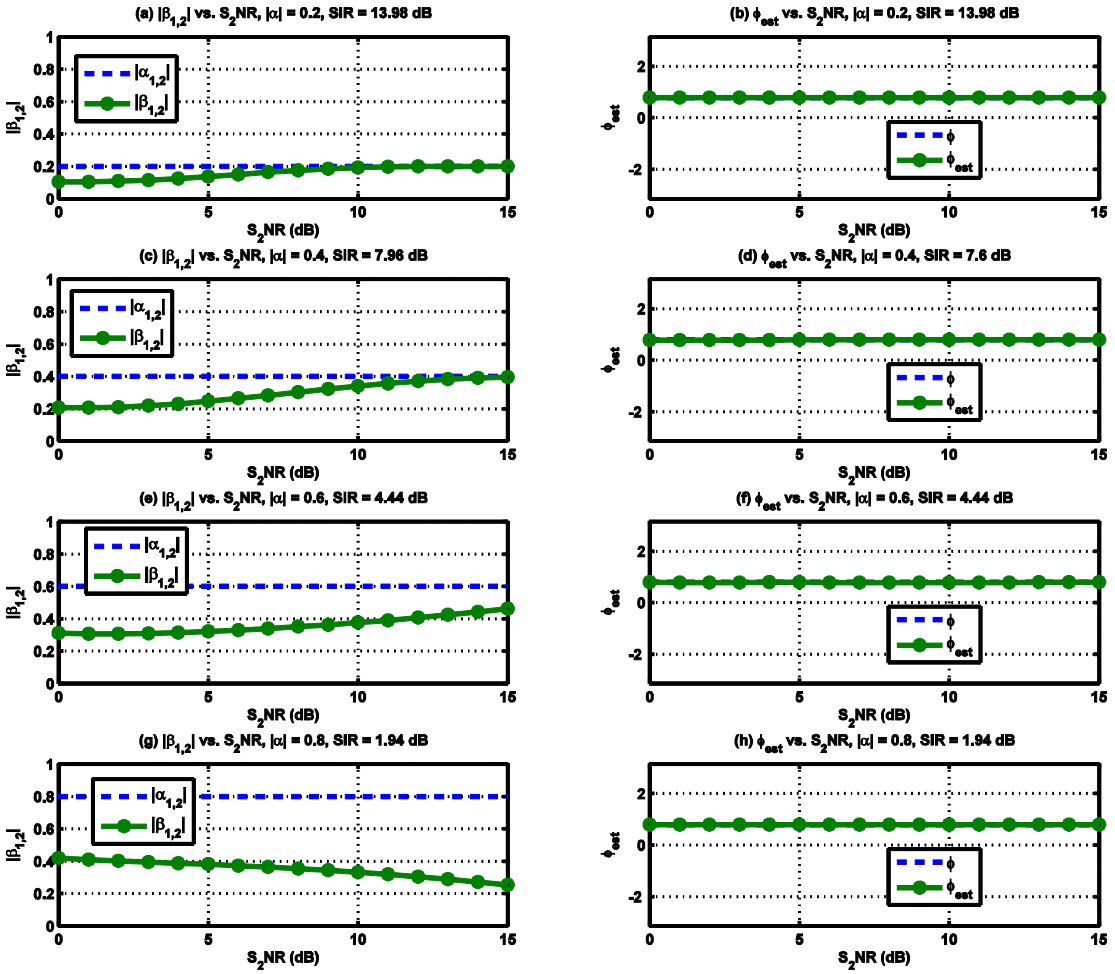

FIGURE 10. Magnitude and phase estimates ($\beta_{1,2}$) vs. S_2NR values for $\alpha_{1,2}$ with $\phi = \pi/4$: (a) magnitude and (b) phase for $|\alpha_{1,2}| = 0.2$; (c) magnitude and (d) phase for $|\alpha_{1,2}| = 0.4$; (e) magnitude and (f) phase for $|\alpha_{1,2}| = 0.6$; and (g) magnitude and (h) phase for $|\alpha_{1,2}| = 0.8$.

natural scope of this paper. Although not necessary, reference transmissions may also be performed at a much later time (since our application of interest is not necessarily latency-limited as already pointed out before).

For Rx_2 (i.e. $m = 1$ interference), we can modify (2) into useful form by replacing $\mathbf{s}_1$ with "first reference" $\hat{\mathbf{s}}_1$. While we may have solved one problem, we still need estimate $\alpha_{1,2}$ which is associated with $\mathbf{s}_1$. But according to (8) estimation requires a priori knowledge of $\mathbf{s}_2$, the very signal it is trying to demodulate which makes for an interesting "Catch-22" problem. Remarkably, RSIC is found to be effective even with this problem! For the time being let's assume we have $\mathbf{s}_2$ or a replacement for it. In Rx_2, estimation is performed. The estimate is applied to the received reference where the scaled version of $\hat{\mathbf{s}}_1$ is subtracted from the received signal $\mathbf{y}_2$. The result is demodulated with the use of MLD yielding $\hat{\mathbf{s}}_2$ (the second reference signal). Rx_2 now transmits this new reference over to Rx_3 (and others). This iteration of cancellation continues for multiple receivers. For example, if $L = 4$, then $\mathbf{s}_4$ is the SoI. In Fig. 1, it is the signal transmitted by BS_4 that Rx_4 (in Sector D) is trying to capture. For a multiple receiver system such as a 4-Rx system, each interferer has a distinct signal strength relative to $\mathbf{s}_4$ as dictated by its amplitude $\alpha_{m,4}$. In other words, each one of these interfering signals contributes to an aggregate signal-to-interference ratio (SIR) that affects the performance of the cancellation technique. The remaining question is: what is the replacement for $\mathbf{s}_n$ in Rx_n such that the estimation can proceed?

C. BREAKING THE "CATCH-22"

For the n^{th}-receiver to perform estimation, we need to solve the issue of the presence of ISM $\mathbf{S} = [\mathbf{s}_1\ \mathbf{s}_2\ \cdots\ \mathbf{s}_{n-1}]$ in (8). Despite possibly containing errors, we utilize the reference signals by stacking the signals in an interference reference matrix (IRM) $\hat{\mathbf{S}} = [\hat{\mathbf{s}}_1\ \hat{\mathbf{s}}_2\ \cdots\ \hat{\mathbf{s}}_{n-1}]$ which becomes our replacement to the true ISM $\mathbf{S} = [\mathbf{s}_1\ \mathbf{s}_2\ \cdots\ \mathbf{s}_{n-1}]$. This resolves one of the two major issues in (8). Unfortunately, we still need to resolve the need in (8) for $\mathbf{s}_n$ which is the very signal Rx_n is trying to demodulate. To solve this problem, we

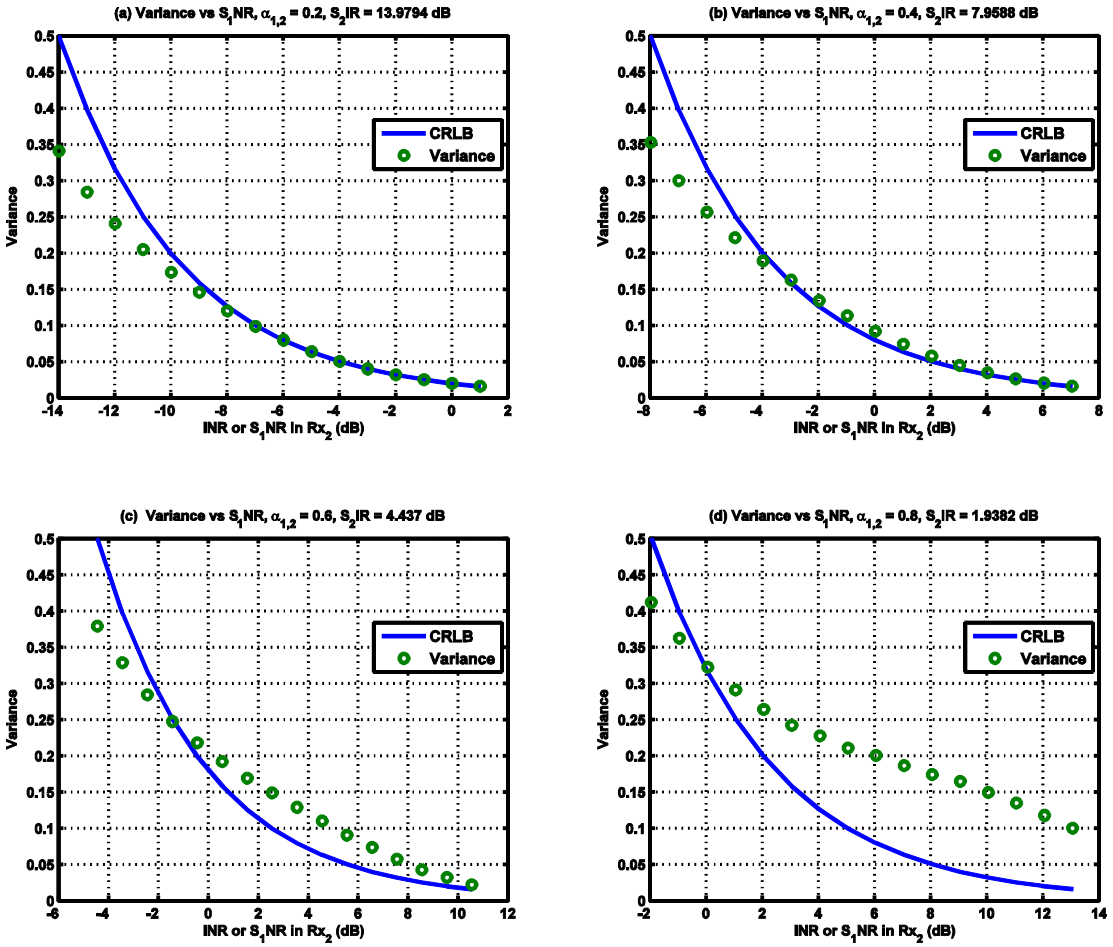

FIGURE 11. The plots of the variance of the estimator $\beta_{1,2}$ vs. S_1NR values: (a) $\alpha_{1,2} = 0.2$, S_2IR = 14 dB; (b) $\alpha_{1,2} = 0.4$, S_2IR = 7.9 dB; (c) $\alpha_{1,2} = 0.6$, S_2IR = 4.4 dB; (d) $\alpha_{1,2} = 0.8$, S_2IR = 1.9 dB.

have to modify (8) and/or (9) in order for them to be useful. We propose to have an initial "guess" on $\mathbf{s}_n$ by preliminarily demodulating the received signal using the standard MLD on $\mathbf{y}_n$ via (3) without using (2). In other words, the first thing the RSIC receiver needs to do is to produce an initial "guess" given by

$$\tilde{\mathbf{s}}_n = \text{dec}(\mathbf{y}_n) = \text{dec}\left(\mathbf{s}_n + \sum_{m=1}^{n-1} \alpha_{m,n}\mathbf{s}_m + \mathbf{w}_n\right) \qquad (10)$$

where it is clear that no prior effort is made to estimate the interferers' amplitudes nor use reference signals in the IRM $\hat{\mathbf{S}} = [\hat{\mathbf{s}}_1\ \hat{\mathbf{s}}_2 \cdots \hat{\mathbf{s}}_{n-1}]$ that may be available. This may sound disconcerting since it is clear that the initial guess may be error-filled depending on the total SIR. Nevertheless, this initial "guess" $\tilde{\mathbf{s}}_n$ is then used along with the rest of the reference signals in $\hat{\mathbf{S}} = [\hat{\mathbf{s}}_1\ \hat{\mathbf{s}}_2 \cdots \hat{\mathbf{s}}_{n-1}]$ to form the vector amplitude estimate where the idealized (8) (which couldn't be used directly) is modified into useful version as given by

$$\boldsymbol{\beta}_n = (\hat{\mathbf{S}}^H\hat{\mathbf{S}})^{-1}\hat{\mathbf{S}}^H\left(\mathbf{y}_n - \tilde{\mathbf{s}}_n\right). \qquad (11)$$

Once amplitude vector is estimated then it can be used to perform the cancellation using a modified and useful version of (2) that allows the use of the IRM which is given by

$$\check{\mathbf{s}}_n = \mathbf{y}_n - \hat{\mathbf{S}}\boldsymbol{\beta}_n \qquad (12)$$

where $\hat{\mathbf{S}}\boldsymbol{\beta}_n = \sum_{m=1}^{n-1} \beta_{m,n}\hat{\mathbf{s}}_m$. Then, we "re-use" MLD in (3) to finally yield the post-demodulated SoI $\hat{\mathbf{s}}_n$. It is clear in (10) that total SIR may be low due to the multitude of interferers and that initial SoI guess (10) is likely to be error-filled especially at low aggregate SIR. Despite this issue, RSIC is proven to work remarkably well in a sense that it is able to correct much of the errors from the interferences. In other words, demodulation of SoI (or multiple SoIs) is shown to be very feasible. Many examples ensue in later sections.

The amplitude estimates are a function of the sum error term in (8). However, which amplitude estimate performs better or worse (and at which SNR or SIR configuration) compared to others is not apparent in (8). We perform Monte Carlo simulations such that we can look at estimation results for various SNR and SIR configurations. Also, the estimates are a function of the number of measurements N. Each sample in $\mathbf{s}_n$ may represent a symbol. For example, if the signal of interest is a communications signal, then a sample can

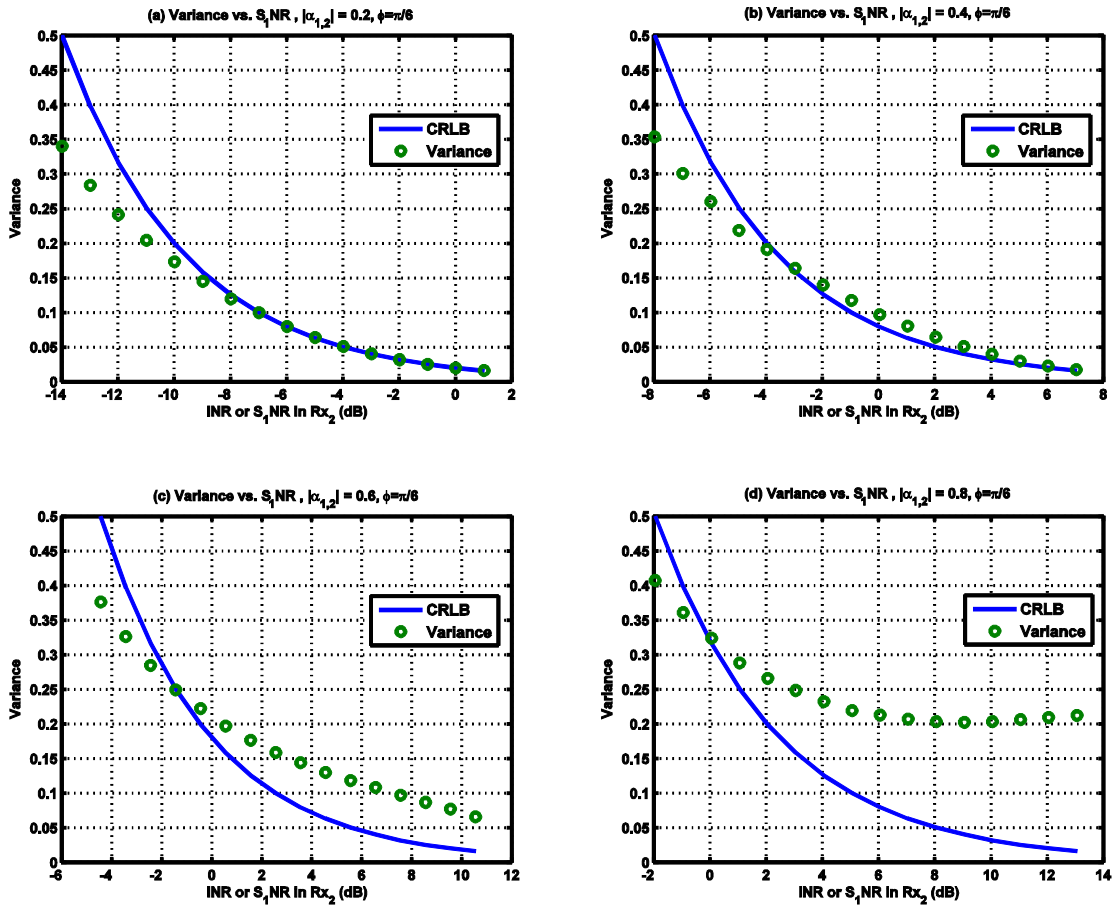

FIGURE 12. The plots of the variance (of the real part) of the estimator $\beta_{1,2}$ vs. S_1NR values for $\alpha_{1,2}$ with $\phi = \pi/6$: (a) $|\alpha_{1,2}| = 0.2$, (b) $|\alpha_{1,2}| = 0.4$, (c) $|\alpha_{1,2}| = 0.6$, and (d) $|\alpha_{1,2}| = 0.8$.

be a symbol. Or each group of N_g samples may represent a symbol. In that case, the total number of symbols in the N-length sequence is $N_s = N/N_g$. For the sake of generating results, we assume that a sample represents a symbol. In signal collection applications where latency is not an issue, it is common to record long data sets and as such N is usually very large. The importance of N (and of it being large) is related to the Cramer-Rao lower bound of the variance of the estimator of the vector $\boldsymbol{\alpha}_n$ which is the topic of the next section.

D. CRAMER-RAO LOWER BOUND (CRLB)

We endeavor to use CRLB in order obtain a lower bound on the variance of our estimator in (8) to determine whether or not the estimator is the mean value unbiased estimator, which may indicate that (8) has the lowest variance of any other unbiased estimator for all possible values of $\boldsymbol{\alpha}_n$. In other words CRLB will be used as a benchmark for comparison. We assume complex baseband signal modeling. Thus the probability density function (*pdf*) of $\mathbf{y}_n$ assuming complex-valued Gaussian noise is given by

$$p(\mathbf{y}_n;\boldsymbol{\alpha}_n) = \frac{1}{\pi^N |\mathbf{C}_n|} \exp\left\{-\left(\mathbf{y}_n - \mathbf{s}_n - \mathbf{S}\boldsymbol{\alpha}_n\right)^H \times \mathbf{C}_n^{-1}\left(\mathbf{y}_n - \mathbf{s}_n - \mathbf{S}\boldsymbol{\alpha}_n\right)\right\} \quad (13)$$

where $\mathbf{C}_n = \sigma^2\mathbf{I}$ is the noise covariance matrix, $\mathbf{C}_n^{-1} = \sigma^{-2}\mathbf{I}$ is its inverse, $\mathbf{I}$ is the identity matrix, and σ^2 is the variance of a sample of the complex-valued additive white Gaussian noise (AWGN) in Rx_n. The log-likelihood yields

$$\begin{aligned}\ln p(\mathbf{y}_n;\boldsymbol{\alpha}_n) &= \ln\left(\frac{1}{\pi^N\sigma^{2N}}\right) \\ &\quad + \ln\exp\left\{-\frac{1}{\sigma^2}\left(\mathbf{y}_n - \mathbf{s}_n - \mathbf{S}\boldsymbol{\alpha}_n\right)^H (y_n - \mathbf{s}_n - \mathbf{S}\boldsymbol{\alpha}_n)\right\} \\ &= \ln\left(\frac{1}{\pi^N\sigma^{2N}}\right) - \frac{1}{\sigma^2}\left(\mathbf{y}_n - \mathbf{s}_n - \mathbf{S}\boldsymbol{\alpha}_n\right)^H\left(\mathbf{y}_n - \mathbf{s}_n - \mathbf{S}\boldsymbol{\alpha}_n\right) \\ &= \ln\left(\frac{1}{\pi^N\sigma^{2N}}\right) - \frac{J(\boldsymbol{\alpha}_n)}{\sigma^2} \end{aligned} \quad (14)$$

where $J(\boldsymbol{\alpha}_n)$ is given in (5).

1) REAL α_n

Taking the first derivative of $\ln p(\mathbf{y}_n;\boldsymbol{\alpha}_n)$ with respect to $\boldsymbol{\alpha}_n$ by using (B2) from the Appendix, we have

$$\frac{\partial \ln p(\mathbf{y}_n;\boldsymbol{\alpha}_n)}{\partial \boldsymbol{\alpha}_n} = \frac{2}{\sigma^2}\left(\mathrm{Re}[\mathbf{S}^H(\mathbf{y}_n - \mathbf{s}_n)] - [\mathrm{Re}(\mathbf{S}^H\mathbf{S})]\boldsymbol{\alpha}_n\right). \quad (15)$$

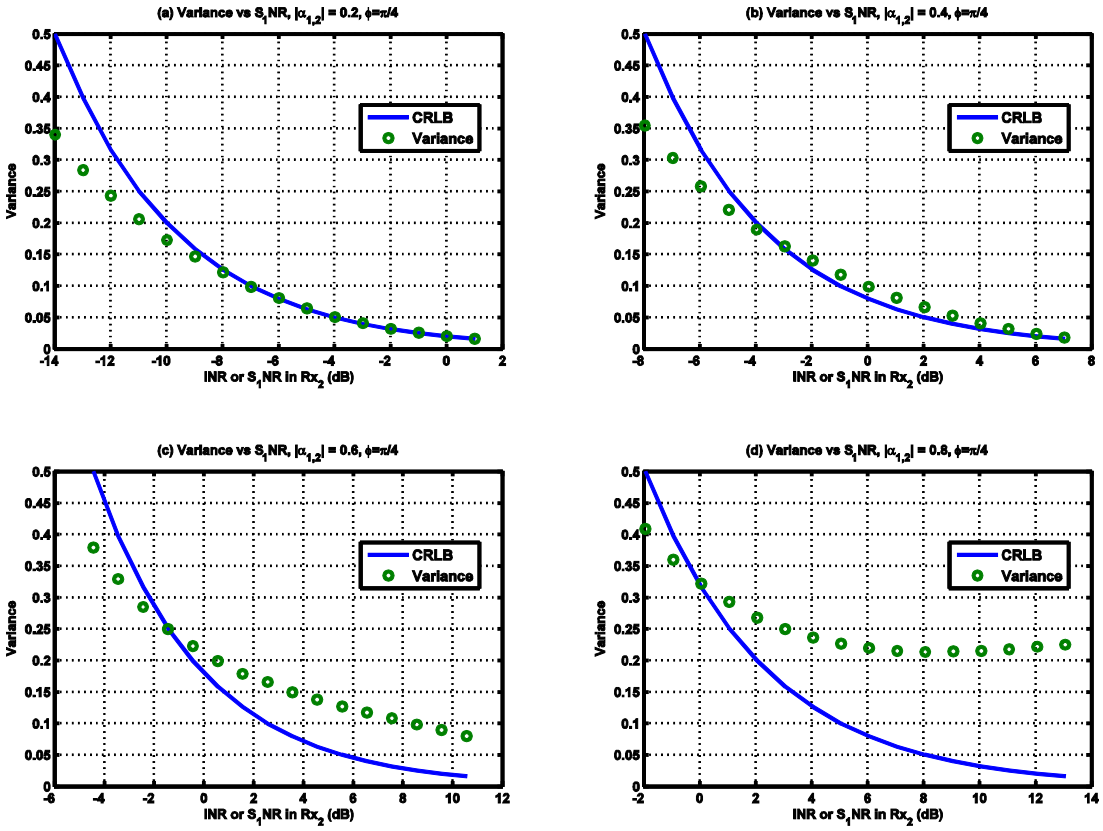

FIGURE 13. The plots of the variance (of the real part) of the estimator $\beta_{1,2}$ vs. S_1NR values for $\alpha_{1,2}$ with $\phi = \pi/4$: (a) $|\alpha_{1,2}| = 0.2$, (b) $|\alpha_{1,2}| = 0.4$, (c) $|\alpha_{1,2}| = 0.6$, and (d) $|\alpha_{1,2}| = 0.8$.

The second vector differentiation results in

$$\frac{\partial^2 \ln p(\mathbf{y}_n;\boldsymbol{\alpha}_n)}{\partial \boldsymbol{\alpha}_n^2} = -\frac{2}{\sigma^2}\mathrm{Re}(\mathbf{S}^H\mathbf{S}) = -\frac{2}{\sigma^2}\mathrm{Re}\begin{bmatrix} \|\mathbf{s}_1\|^2 & \mathbf{s}_1^H\mathbf{s}_2 & \dots & \mathbf{s}_1^H\mathbf{s}_{n-1} \\ \mathbf{s}_2^H\mathbf{s}_1 & \|\mathbf{s}_2\|^2 & \dots & \mathbf{s}_2^H\mathbf{s}_{n-1} \\ \vdots & \vdots & \ddots & \vdots \\ \mathbf{s}_{n-1}^H\mathbf{s}_1 & \mathbf{s}_{n-1}^H\mathbf{s}_1 & \dots & \|\mathbf{s}_{n-1}\|^2 \end{bmatrix}. \tag{16}$$

Then the Fisher information matrix (FIM) is given by

$$\mathbf{I}(\boldsymbol{\alpha}_n) = -\mathrm{E}\left[\frac{\partial^2 \ln p(\mathbf{y}_n;\boldsymbol{\alpha}_n)}{\partial \boldsymbol{\alpha}_n^2}\right] \tag{17}$$

where E[*] is the expected value operator and thus

$$\mathbf{I}(\boldsymbol{\alpha}_n) = \frac{2}{\sigma^2}\mathrm{E}\left(\mathrm{Re}\begin{bmatrix} \|\mathbf{s}_1\|^2 & \mathbf{s}_1^H\mathbf{s}_2 & \dots & \mathbf{s}_1^H\mathbf{s}_{n-1} \\ \mathbf{s}_2^H\mathbf{s}_1 & \|\mathbf{s}_2\|^2 & \dots & \mathbf{s}_2^H\mathbf{s}_{n-1} \\ \vdots & \vdots & \ddots & \vdots \\ \mathbf{s}_{n-1}^H\mathbf{s}_1 & \mathbf{s}_{n-1}^H\mathbf{s}_1 & \dots & \|\mathbf{s}_{n-1}\|^2 \end{bmatrix}\right) \tag{18}$$

which reduces to

$$\mathbf{I}(\boldsymbol{\alpha}_n) = \frac{2N}{\sigma^2}\begin{bmatrix} \overline{E}_{s_1} & \rho_{1,2} & \dots & \rho_{1,n-1} \\ \rho_{2,1} & \overline{E}_{s_2} & \dots & \rho_{2,n-1} \\ \vdots & \vdots & \ddots & \vdots \\ \rho_{n-1,1} & \rho_{n-1,2} & \dots & \overline{E}_{s_{n-1}} \end{bmatrix} \tag{19}$$

where $\overline{E}_s$ is the average energy of a symbol (sample) in the data sequence and $\rho_{k,l} = \frac{1}{N}\mathrm{E}\left[\mathrm{Re}(\mathbf{s}_k^H\mathbf{s}_l)\right]$. For constant energy modulations, the average symbol energy is simply equal to symbol energy. In our examples, we use QPSK and as such $\overline{E}_s = E_s$. Finally, the CRLB of an amplitude estimate which is the reciprocal of a diagonal in the FIM is given by

$$\mathrm{var}(\beta_{m,n}) \geq \frac{\sigma^2}{2\bar{E}_s N}. \tag{20}$$

In other words, the CRLB is inversely proportional to the average SNR and the number of symbols. The larger the SNR, the smaller is the CRLB. The longer the symbol sequence, the smaller is the CRLB.

Although not true in general, the data sequence may be uncorrelated from one emitter to another emitter or at least not very correlated. This may be a practical assumption when the emitters are not co-located and thus are isolated from each other. Moreover, if the generation of data from one emitter to emitter is truly independent, then off-diagonal elements in the FIM are zero. For this special case, the FIM reduces to

$$\mathbf{I}(\boldsymbol{\alpha}_n) = \frac{2N}{\sigma^2}\begin{bmatrix} \overline{E}_{s_1} & 0 & \dots & 0 \\ 0 & \overline{E}_{s_2} & \dots & 0 \\ \vdots & \vdots & \ddots & \vdots \\ 0 & 0 & \dots & \overline{E}_{s_{n-1}} \end{bmatrix}. \tag{21}$$

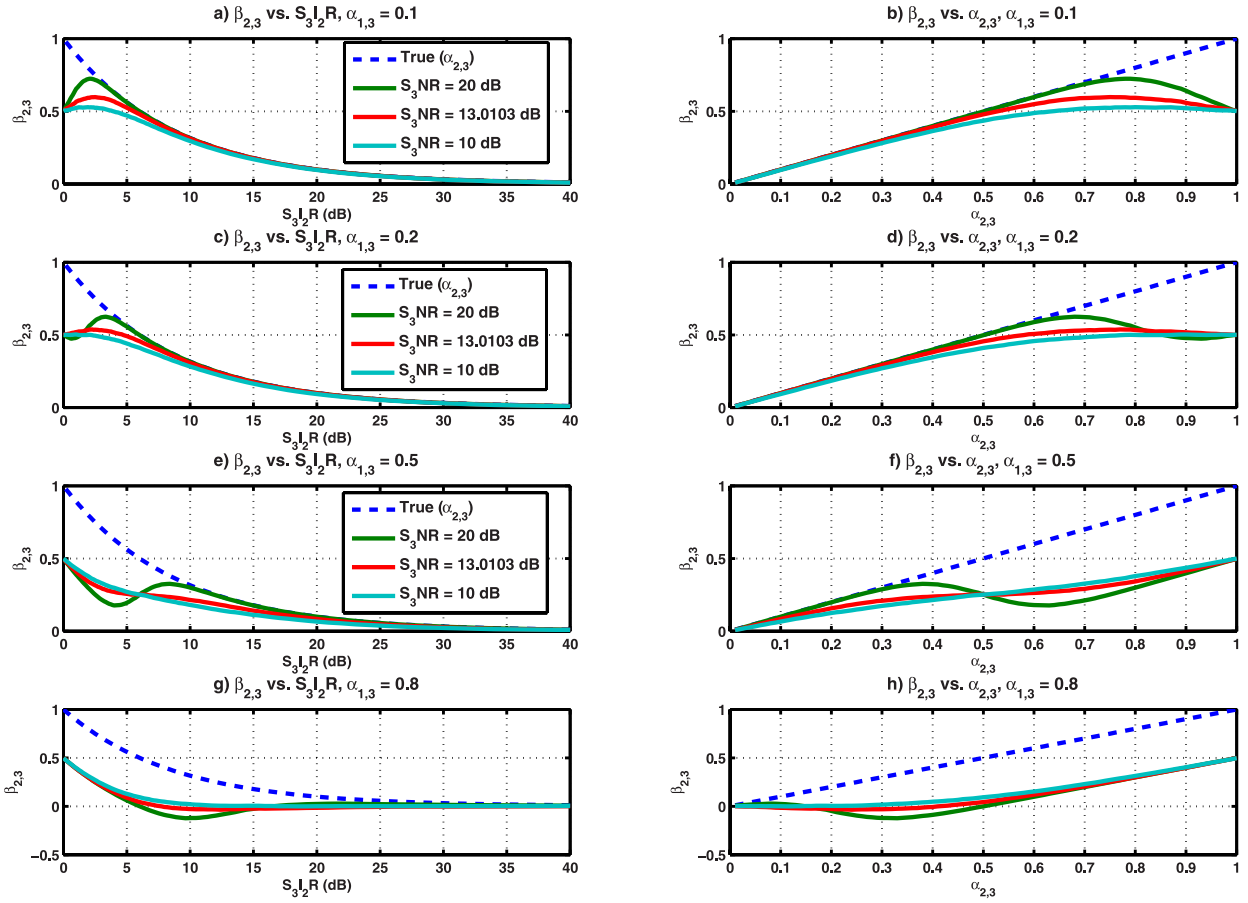

FIGURE 14. The plots of amplitude estimates $\beta_{2,3}$ vs. S_3I_2R values with fixed high S_3NR levels: (a)–(b) $\alpha_{1,3} = 0.1$; (c)–(d) $\alpha_{1,3} = 0.2$; (e)–(f) $\alpha_{1,3} = 0.5$; (g)–(h) $\alpha_{1,3} = 0.8$.

Recall that the ISM $\mathbf{S}$ is not truly available. Instead, when we calculate variances to compare to (20), we use signal matrix $\hat{\mathbf{S}}$. In other words, we compare the calculated variances to that of the CRLB given by (20). Although relatively clean, the reference (interfering) signals in $\hat{\mathbf{S}}$ are "estimates" themselves (i.e. hard detections) in the sense they have accumulated errors. The first set of errors comes from the demodulation of the references from the receivers. The second set of errors comes from receiving the transmitted references in the subsequent receivers. In our simulations, we assume sufficient to high SNR in the latter such that most (if not all) the errors come from the former. These accumulated errors may contribute to the actual calculated covariance matrix of the estimates. In summary, the actual covariance matrix of the estimate may not only depend on the noise and energy of the signal corresponding to the amplitude but also depend on how much error is in the reference signals.

2) COMPLEX α_n

When the estimates are complex-valued, it is more convenient to start with the FIM to find the CRLB. It is known [14], [15] that the FIM or more specifically the individual entry of the FIM is given by

$$[\mathbf{I}(\boldsymbol{\alpha}_n)]_{kl} = \mathrm{Tr}\left[\mathbf{C}_n^{-1}(\boldsymbol{\alpha}_n)\frac{\partial \mathbf{C}_n(\boldsymbol{\alpha}_n)}{\partial \boldsymbol{\alpha}_{n,k}}\mathbf{C}_n^{-1}(\boldsymbol{\alpha}_n)\frac{\partial \mathbf{C}_n(\boldsymbol{\alpha}_n)}{\partial \boldsymbol{\alpha}_{n,l}}\right] + 2\mathrm{Re}\left[\frac{\partial \boldsymbol{\mu}_n^H(\boldsymbol{\alpha}_n)}{\partial \boldsymbol{\alpha}_{n,k}}\mathbf{C}_n^{-1}(\boldsymbol{\alpha}_n)\frac{\partial \boldsymbol{\mu}_n(\boldsymbol{\alpha}_n)}{\partial \boldsymbol{\alpha}_{n,l}}\right] \quad (22)$$

where k and l denote the location of the individual entry of the FIM, Tr[*] stands for the "trace" operator and $\boldsymbol{\mu}_n(\boldsymbol{\alpha}_n) = \mathbf{s}_n + \mathbf{S}\boldsymbol{\alpha}_n$ using (13). Since $\mathbf{C}_n = \sigma^2\mathbf{I}$, the first term is clearly zero. We have

$$[\mathbf{I}(\boldsymbol{\alpha}_n)]_{kl} = \frac{1}{\sigma^2}2\mathrm{Re}\left[\frac{\partial \boldsymbol{\mu}_n^H(\boldsymbol{\alpha}_n)}{\partial \boldsymbol{\alpha}_{n,k}}\frac{\partial \boldsymbol{\mu}_n(\boldsymbol{\alpha}_n)}{\partial \boldsymbol{\alpha}_{n,l}}\right]. \quad (23)$$

Using the definition of the complex gradient, we have

$$\frac{\partial \boldsymbol{\mu}_n(\boldsymbol{\alpha}_n)}{\partial \boldsymbol{\alpha}_n} = \frac{1}{2}\left[\frac{\partial}{\partial \boldsymbol{\alpha}_{n,r}}(\mathbf{s}_n + \mathbf{S}\boldsymbol{\alpha}_n) - j\frac{\partial}{\partial \boldsymbol{\alpha}_{n,i}}(\mathbf{s}_n + \mathbf{S}\boldsymbol{\alpha}_n)\right] \quad (24)$$

where $\boldsymbol{\alpha}_{n,r}$ refers to the real part of $\boldsymbol{\alpha}_n$ and $\boldsymbol{\alpha}_{n,i}$ refers to the imaginary part. Then,

$$\frac{\partial}{\partial \boldsymbol{\alpha}_{n,r}}\left(\mathbf{s}_{n,r} + j\mathbf{s}_{n,i} + \mathbf{S}\boldsymbol{\alpha}_{n,r} + j\mathbf{S}\boldsymbol{\alpha}_{n,i}\right) = \mathbf{S} \quad (25)$$

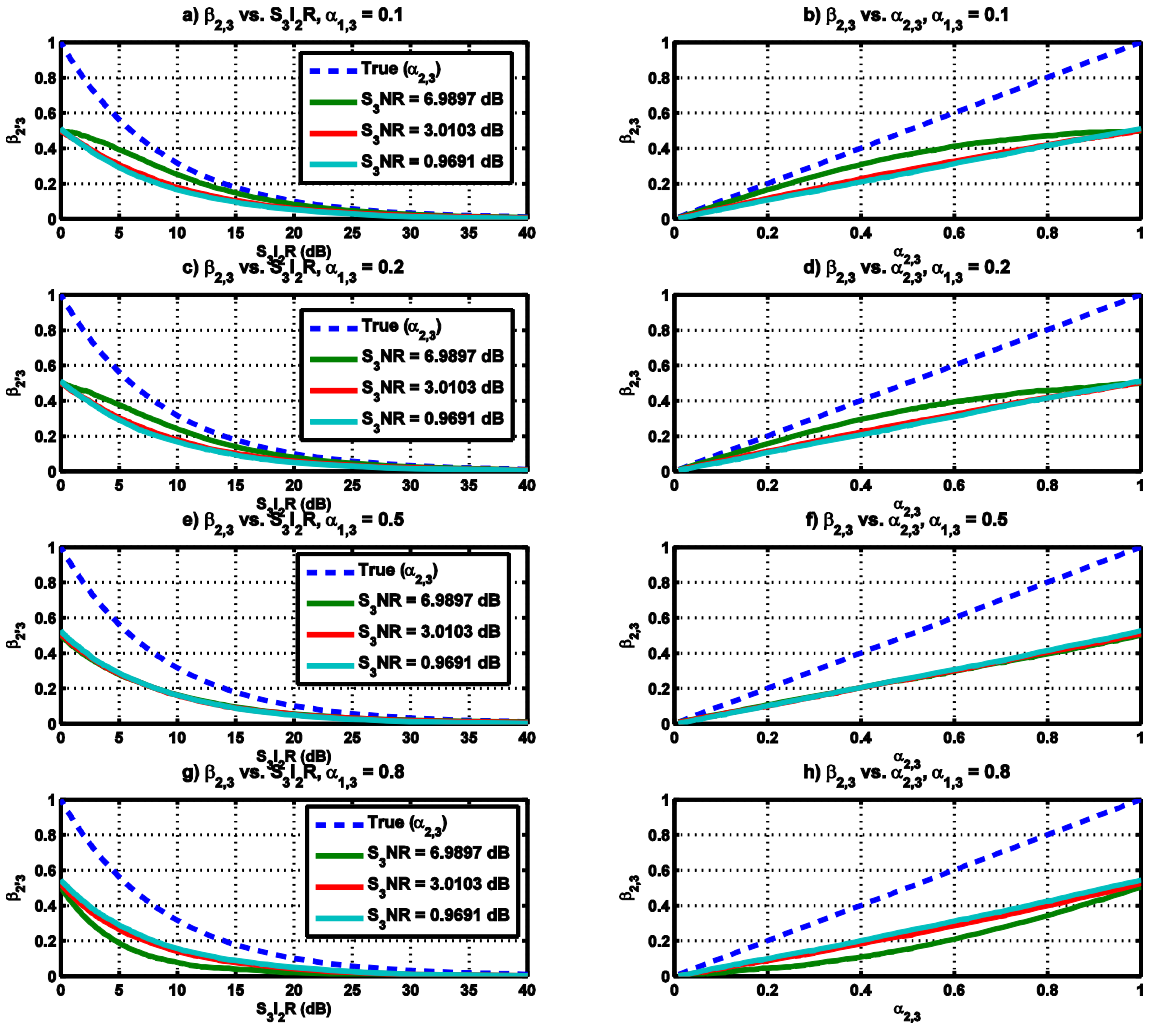

FIGURE 15. The plots of amplitude estimates $\beta_{2,3}$ vs. S_3I_2R values with fixed low S_3NR levels: (a)–(b) $\alpha_{1,3} = 0.1$; (c)–(d) $\alpha_{1,3} = 0.2$; (e)–(f) $\alpha_{1,3} = 0.5$; (g)–(h) $\alpha_{1,3} = 0.8$.

where $\mathbf{s}_{n,r}$ and $\mathbf{s}_{n,i}$ refer to the real and complex part of $\mathbf{s}_n$ respectively. It follows that

$$\frac{\partial}{\partial \boldsymbol{\alpha}_{n,i}}\left(\mathbf{s}_{n,r} + j\mathbf{s}_{n,i} + \mathbf{S}\boldsymbol{\alpha}_{n,r} + j\mathbf{S}\boldsymbol{\alpha}_{n,i}\right) = j\mathbf{S}. \tag{26}$$

Also,

$$\frac{\partial \boldsymbol{\mu}_n(\boldsymbol{\alpha}_n)}{\partial \boldsymbol{\alpha}_n} = \frac{1}{2}\left[\mathbf{S} - j(j\mathbf{S})\right] = \mathbf{S}. \tag{27}$$

In view of (23), then any diagonal element of the FIM is given by

$$[\mathbf{I}(\boldsymbol{\alpha}_n)]_{kk} = \frac{1}{\sigma^2} 2\mathrm{Re}\left[\mathbf{s}_k^H \mathbf{s}_k\right] = \frac{2\|\mathbf{s}_k\|^2}{\sigma^2} = \frac{2N\bar{E}_s}{\sigma^2}. \tag{28}$$

In other words, the CRLB of a complex-valued estimate is given by

$$\mathrm{var}(\beta_{m,n}) \geq \frac{1}{2N\frac{\bar{E}_s}{\sigma^2}} = \frac{\sigma^2}{2\bar{E}_s N}. \tag{29}$$

III. TWO-RECEIVER SYSTEM

For a two-receiver system, the reference is given by $\hat{\mathbf{s}}_1 = \mathrm{dec}(\mathbf{y}_1)$ and the initial SoI guess is $\tilde{\mathbf{s}}_2 = \mathrm{dec}(\mathbf{y}_2)$. Then,

$$\beta_{1,2} = (\hat{\mathbf{s}}_1^H \hat{\mathbf{s}}_1)^{-1} \hat{\mathbf{s}}_1^H \left(\mathbf{y}_2 - \tilde{\mathbf{s}}_2\right). \tag{30}$$

If $\alpha_{1,2}$ is real, then the estimate is given by

$$\beta_{1,2} = [\mathrm{Re}(\hat{\mathbf{s}}_1^H \hat{\mathbf{s}}_1)]^{-1} \mathrm{Re}[\hat{\mathbf{s}}_1^H (\mathbf{y}_2 - \tilde{\mathbf{s}}_2)]. \tag{31}$$

The reference $\hat{\mathbf{s}}_1$ is scaled by $\beta_{1,2}$ and is subtracted from the received signal to demodulate Rx_2 SoI which is given by $\hat{\mathbf{s}}_2 = \mathrm{dec}(\mathbf{y}_2 - \beta_{1,2}\hat{\mathbf{s}}_1)$. The following sections show various simulation SER and estimation results.

A. ESTIMATION RESULTS: PARAMETERIZE S_2NR, VARY $\alpha_{1,2}$

It turns out estimation plays a vital role in the SER performance of the RSIC technique. As such, it is important to explore how the estimates perform as the true parameter is varied given SNR. Since $\mathbf{y}_2$ is made up of SoI $\mathbf{s}_2$ and the scaled

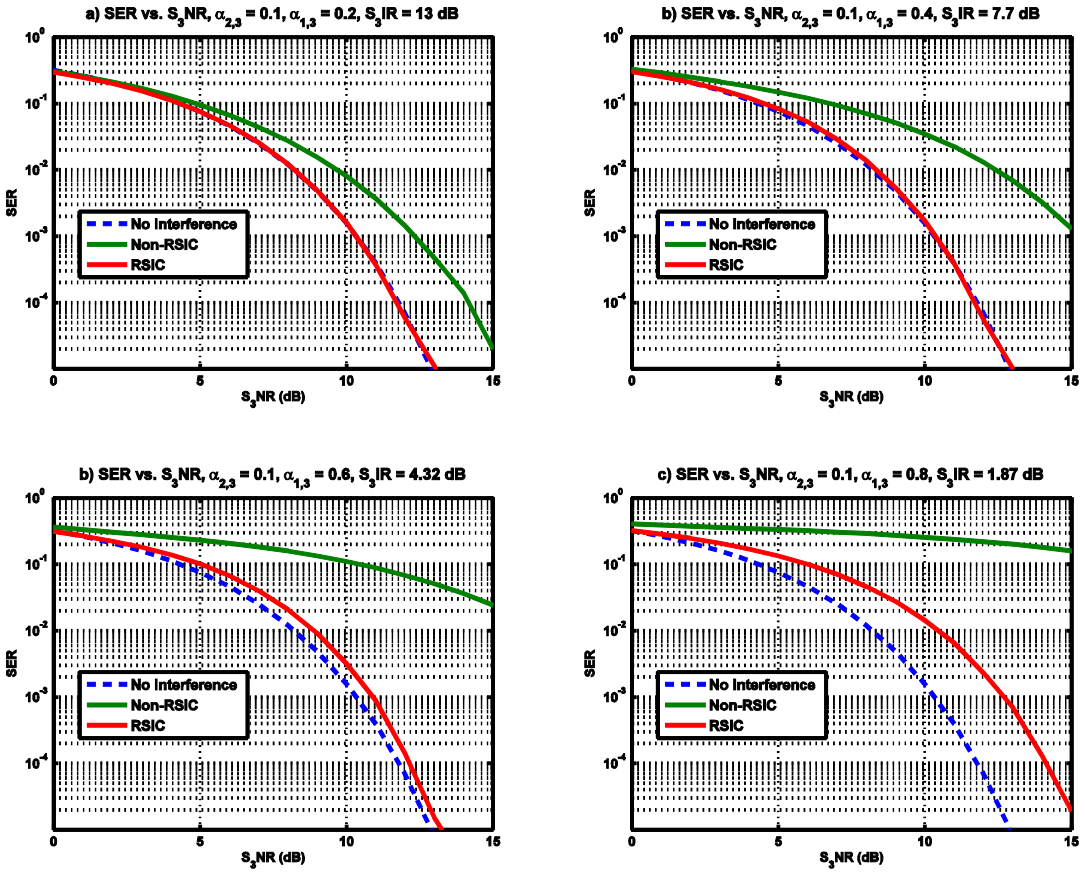

FIGURE 16. The performance curves of SER vs. S_3NR for demodulation of SoI s_3 in Rx3 at different interference combinations when $\alpha_{2,3} = 0.1$: (a) $\alpha_{1,3} = 0.2$, S_3IR = 13 dB; (b) $\alpha_{1,3} = 0.4$, S_3IR = 7.7 dB; (c) $\alpha_{1,3} = 0.6$, S_3IR = 4.32 dB; (d) $\alpha_{1,3} = 0.8$, S_3IR = 1.87 dB.

interference $\mathbf{s}_1$, the SIR is therefore defined as

$$S_2\text{IR} \triangleq \frac{E_{\mathbf{s}_2}}{E_{\mathbf{s}_1}} = \frac{\|\mathbf{s}_2\|^2}{\|\alpha_{1,2}\mathbf{s}_1\|^2} \tag{32}$$

where $E_{\mathbf{s}_i}$, $i = 1, 2$ are the sequence energies of amplitude-scaled interference $\mathbf{s}_1$ and SoI $\mathbf{s}_2$. We use QPSK modulation for our simulations and as such the SIR simplifies to

$$S_2\text{IR} = \frac{1}{|\alpha_{1,2}|^2}. \tag{33}$$

In our Monte Carlo simulations (1×10^6 QPSK symbols for each $\mathbf{s}_1$ and $\mathbf{s}_2$ data stream), the SNR of the SoI $\mathbf{s}_2$ is varied by simply changing the noise variance or power P_n in the received signals. The 1×10^6 symbols is in anticipation of generating SER results that are good to SER of about 1×10^{-5}. For convenience, let's start with $\alpha_{1,2}$ being real and positive (i.e. symbols are synchronized in time prior to demodulation). The values of $\alpha_{1,2}$ are varied from 0.01 to 1.0 to vary the S_2IR given a signal-to-noise ratio, or S_2NR. We then vary the S_2NR to observe the effect on the estimate $\beta_{1,2}$ compared to the actual amplitude $\alpha_{1,2}$. Because of the inverse relationship in (33), as $\alpha_{1,2}$ is increased the value of S_2IR decreases. Initially, P_n is set low in order to model a system where there is high S_2NR. We then increase P_n gradually to model low S_2NR. The comparison (sometimes referred to as "tightness" or "closeness") between the estimate $\beta_{1,2}$ and the amplitude $\alpha_{1,2}$ for various SNR is shown in Fig. 2a (high S_2NR) and Fig. 2b (low S_2NR). We see that the dashed blue line represents the actual $\alpha_{1,2}$ parameters used in the simulation. At high S_2NR level of 20 dB, the calculated estimate $\beta_{1,2}$ values are close to $\alpha_{1,2}$ until $\alpha_{1,2}$ takes on the value of 0.8 to 1.0 (significant interference). The value 0.8 corresponds to a very low S_2IR (about 2 dB). In other words, the amplitude estimate is still good at low S_2IR (about 2 dB) but at a high S_2NR (20 dB). If the noise is increased (i.e. low S_2NR), the "closeness" (which indicates accuracy) of the estimator to the actual parameter begins to deviate as shown in Fig. 2b. At a modest S_2NR of 6.99 dB, the estimator may be considered reasonable at $S_2\text{IR} \geq 15$dB. At a very low $S_2\text{NR} = 0.97$ dB, the estimates do not get close to the true value unless values of $\alpha_{1,2}$ are very small. Interestingly as $\alpha_{1,2}$ gets larger, the estimate gets worse; it begins to converge towards the value of 0.5. It seems that estimator from (31) is more accurate for systems where $||\mathbf{s}_2||^2 \gg |\alpha_{1,2}|^2||\mathbf{s}_1||^2$. Thus, the estimator does not yield good estimates for high $\alpha_{1,2}$ levels at least when the "initial guess" in (10) is used.

Another useful way to see how effective the estimates are ($\beta_{1,2}$) is to plot them against the actual $\alpha_{1,2}$ parameter values as shown in Fig. 2c (high S_2NR) and Fig. 2d (low S_2NR). Again, the dashed blue line represents actual

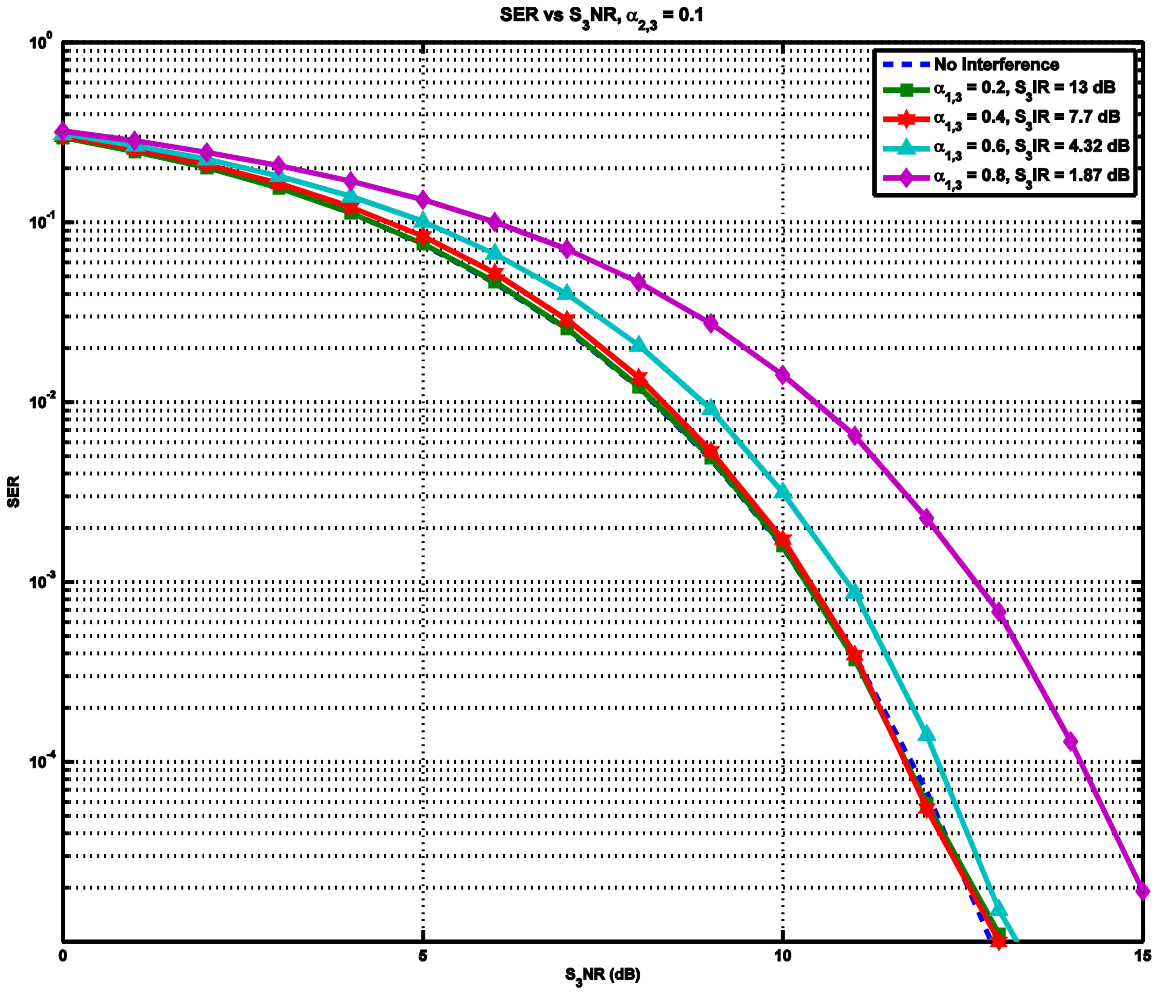

FIGURE 17. The RSIC performance curves of SER vs. S_3NR for demodulation of SoI s_3 in Rx_3 as a function of increasing $\alpha_{1,3}$ with $\alpha_{2,3} = 0.1$.

amplitude parameter $\alpha_{1,2}$ values and the subsequent curves show the estimates at various S_2NRs. At low P_n levels, the estimates are fairly accurate until $\alpha_{1,2}$ is about 0.8 (or greater) as observed before. At higher $\alpha_{1,2}$ values, the estimates deviate far from the actual amplitude. Thus, we can appreciate the joint effect of varying noise and varying interference on the amplitude estimates.

A more general scenario is where $\alpha_{1,2}$ is complex-valued. The values of $|\alpha_{1,2}|$ are varied from 0.01 to 1.0 to vary the S_2IR given a fixed S_2NR and we let the phase of any $\alpha_{1,2}$ be $\phi = \pi/6 = 30°$. Again, we vary the S_2NR to observe the effect on the magnitude and phase estimate of $\beta_{1,2}$ compared to the magnitude and phase of $\alpha_{1,2}$. The comparison between the magnitudes and phases of $\beta_{1,2}$ compared to $\alpha_{1,2}$ are shown in Fig. 3a, 3b, and 3c for high S_2NR and Fig. 3d, 3e, and 3f for low S_2NR. The magnitude estimate results somewhat mirror that of $\alpha_{1,2}$ being real. The main difference between the $\alpha_{1,2}$ being real and complex is that the complex-valued estimate has a phase component where it is clear that at very low S_2IR ($0< S_2\text{IR}<3$dB), the phase estimates are definitely not as good compared to phase estimates with high S_2IR. What's interesting however is that the "poor" phase estimates for $0< S_2\text{IR}<3$dB are worse for high SNR than low SNR; which is a result not readily apparent from (8). Thus, this is where simulation results become very useful.

It is also of interest to see the effect of increasing the phase offset. Since QPSK is phase modulated, the received phase may in fact affect demodulation as well as estimation. We again vary $|\alpha_{1,2}|$ from 0.01 to 1.0 and let the phase of any $\alpha_{1,2}$ be $\phi = \pi/4 = 45°$ which means that the received constellation symbols are shifted by half a symbol which would make symbol demodulation even more erroneous if not corrected. Again, we also vary the S_2NR. The comparison between the magnitudes and phases of $\beta_{1,2}$ compared to $\alpha_{1,2}$ is shown in Fig. 4a, 4b, and 4c for high S_2NR and Fig. 4d, 4e, and 4f for low S_2NR. Although the performance trends are similar, we note that in terms of amplitude and phase estimates, there are some interesting differences for $\phi = \pi/6$ and $\phi = \pi/4$. Looking at Fig. 3a and Fig. 4a, we note that for $S_2\text{NR} = 10$ dB and $S_2\text{IR} = 5$dB where $|\alpha_{1,2}| = 0.56$, the estimate for $\phi = \pi/6$ is $|\beta_{1,2}| = 0.4$ while for $\phi = \pi/4$ is $|\beta_{1,2}| = 0.38$ which means that

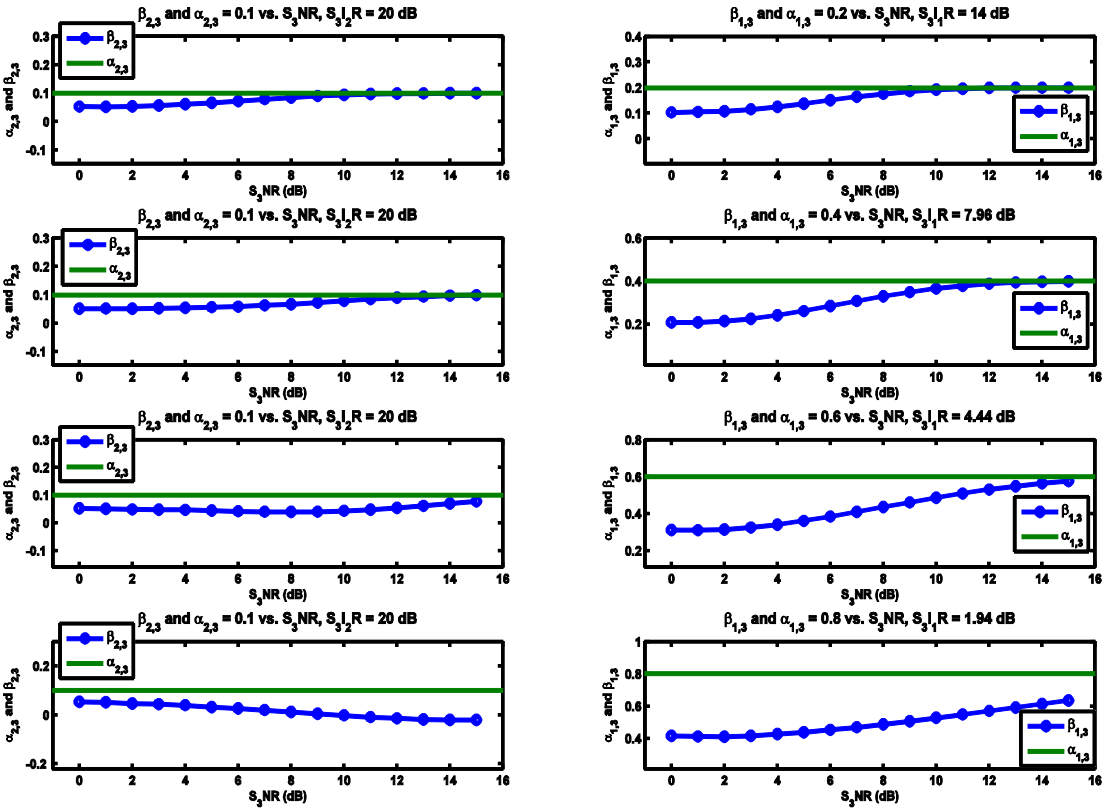

FIGURE 18. Receiver 3 estimates ($\beta_{2,3}$ and $\beta_{1,3}$) and actual parameters ($\alpha_{2,3}$ and $\alpha_{1,3}$) vs. S_3NR for $\alpha_{2,3} = 0.1$ which is paired with: $\alpha_{1,3} = 0.2$, 0.4, 0.6, and 0.8.

the phase increase does have an effect on the magnitude estimate (in this case a slight degradation). Looking at the corresponding phase estimates in Fig. 3b and Fig. 4b, we can see that phase estimate is closer to the actual parameter in the case of $\phi = \pi/4$. In other words it is very interesting to note that at low SIR, the magnitude estimates are better in the case of $\phi = \pi/6$ but phase estimates are better in the case of $\phi = \pi/4$, which is another result that is not intuitive from (8) and would not have been known if not for the simulations.

1) DEMODULATION (SER) RESULTS: PARAMETERIZE $\alpha_{1,2}$, VARY S_2NR

While it is certainly interesting to discuss the amplitude (magnitude and phase) estimation results, we emphasize that our main interest is signal collection where faithful demodulation of SoI is of importance. Since the SoIs in our examples are communications signals, SER (or BER as in bit error rate) performance naturally becomes the metric of interest. We set up an experiment where we generate $\mathbf{s}_1$ that is received by Rx_1. Since we assume the initial signal is to be received with sufficient or high SNR, we assume a 20 dB S_1NR in Rx_1 in our simulations where demodulation results in reference $\hat{\mathbf{s}}_1$. To show SoI ($\mathbf{s}_2$) SER vs S_2NR in Rx_2, we hold the interference amplitude constant $\alpha_{1,2}$ while the noise power is varied. Then we vary $\alpha_{1,2}$ for various S_2IR scenarios. Here, we assume $\alpha_{1,2}$ to be real and positive (the case of complex-valued $\alpha_{1,2}$ is considered next). We show the SER vs S_2NR in: Fig. 5a) $\alpha_{1,2} = 0.2$, S_2IR = 14 dB; Fig. 5b) $\alpha_{1,2} = 0.4$, S_2IR = 7.96 dB; Fig. 5c) $\alpha_{1,2} = 0.6$, S_2IR = 4.4 dB; and Fig. 5d) $\alpha_{1,2} = 0.8$, S_2IR = 1.94 dB. In Fig. 5, the dashed blue line represents the theoretical QPSK SER over noise (i.e. interference-free) via the use of standard maximum-likelihood (MLD) detector (thus labeled 'No interference'). The line labeled 'Non-RSIC' corresponds to the SoI SER performance with interference (amplitude $\alpha_{1,2} = 0.2$ in Fig. 5a) employing MLD where $\tilde{\mathbf{s}}_2 = \text{dec}(\mathbf{y}_2)$. As expected the Non-RSIC SER is degraded compared to the interference-free SER. For example, the Non-RSIC SER is 1.2×10^{-4} at S_2NR = 13dB compared to 8×10^{-6} if there were no interference. To implement RSIC, recall that we first have to estimate $\alpha_{1,2}$ via $\beta_{1,2} = [\text{Re}(\hat{\mathbf{s}}_1^H \hat{\mathbf{s}}_1)]^{-1}\text{Re}[\hat{\mathbf{s}}_1^H(\mathbf{y}_2 - \tilde{\mathbf{s}}_2)]$ which uses $\tilde{\mathbf{s}}_2$. Then, the resulting demodulated signal is given by $\hat{\mathbf{s}}_2 = \text{dec}(\mathbf{y}_2 - \beta_{1,2}\hat{\mathbf{s}}_1)$ in which the SER curve is labeled 'RSIC' in Fig. 5a. The RSIC SER performance is vastly improved compared to the Non-RSIC where SER remarkably approaches the interference-free QPSK SER. In Fig. 5b we illustrate the Non-RSIC SER with $\alpha_{1,2} = 0.4$ (S_2IR = 7.96 dB) and we note that the SER is 3.7×10^{-3} at S_2NR = 13 dB (again compared to 8×10^{-6} if there were no interference) while the RSIC SER again approaches the interference-free SER. In Fig. 5c we illustrate the Non-RSIC SER where $\alpha_{1,2} = 0.6$ (S_2IR = 4.44 dB) and we note that the SER is 3.7×10^{-2} at S_2NR = 13 dB (which is unacceptable in most systems). The RSIC SER (1.7×10^{-5})

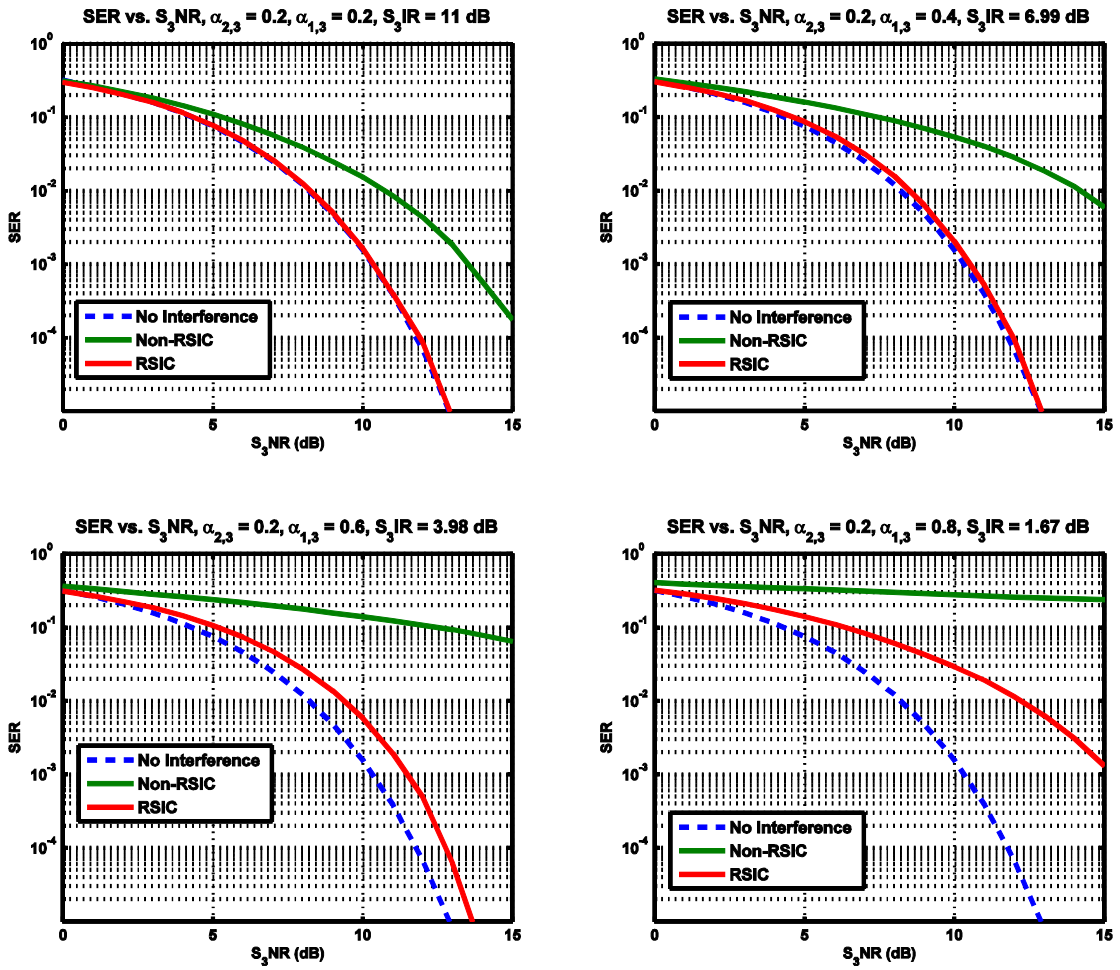

FIGURE 19. The performance curves of SER vs. S_3NR for demodulation of SoI s_3 in Rx3 at different interference combinations when $\alpha_{2,3} = 0.2$: (a) $\alpha_{1,3} = 0.2$, S_3IR = 11 dB; (b) $\alpha_{1,3} = 0.4$, S_3IR = 6.99 dB; (c) $\alpha_{1,3} = 0.6$, S_3IR = 3.98 dB; (d) $\alpha_{1,3} = 0.8$, S_3IR = 1.67 dB.

is close to the interference-free SER of 8×10^{-6} which is 3 decades better than the Non-RSIC SER. We can also look at the improvement in terms of S_2NR savings. For example, the Non-RSIC SER of about 1×10^{-2} corresponds to approximately 15dB of S_2NR while for the RSIC it is approximately 9dB, i.e. a 6dB SNR savings! In other words, the proposed RSIC technique works very well. In Fig. 5d we illustrate the Non-RSIC SER where $\alpha_{1,2} = 0.8$ (S_2IR = 1.94 dB) and we note that the non-RSIC performance is 1.7×10^{-2} at S_2NR = 13 dB which is terribly degraded. The RSIC SER performance at the same SNR is 1.4×10^{-4} which is two decades of SER improvement despite the large interference.

Now we consider the case where $\alpha_{1,2}$ is complex. We allow the phase offset $\phi = \pi/6$ where $\alpha_{1,2} = 0.2^{j\pi/6}$, $0.4^{j\pi/6}$, $0.6^{j\pi/6}$, $0.8^{j\pi/6}$. We show the SER vs S_2NR in Fig.: 6a) $|\alpha_{1,2}| = 0.2$, S_2IR = 14 dB; 6b) $|\alpha_{1,2}| = 0.4$, S_2IR = 7.96 dB; 6c) $|\alpha_{1,2}| = 0.6$, S_2IR = 4.4 dB; and 6d) $|\alpha_{1,2}| = 0.8$, S_2IR = 1.94 dB. The SER without the use of RSIC suffers as a function of increasing $|\alpha_{1,2}|$ but the interesting fact to note is for the case where there is a phase offset of 30 deg, the Non-RSIC SER performance is worse than when the phase offset is 0 ($\alpha_{1,2}$ is real where we recall the SER performances are shown in Fig. 5). We also note the effectiveness of the RSIC method. For the cases of $\alpha_{1,2} = 0.2^{j\pi/6}, 0.4^{j\pi/6}$, the RSIC SERs approach the interference-free SER while the SER for $\alpha_{1,2} = 0.6^{j\pi/6}$ is still close to the interference-free SER (albeit slightly worse than the SER for $\alpha_{1,2} = 0.6$ in Fig. 5c). For the case of $\alpha_{1,2} = 0.8^{j\pi/6}$ RSIC SER is still better than the Non-RSIC but comparatively worse than SER for $\alpha_{1,2} = 0.8$ in Fig. 5d. In other words, the SER effect of phase offset is significant when the interference is also significant.

We mention that another interesting choice for the phase offset is $\phi = \pi/4$ where $\alpha_{1,2} = 0.2^{j\pi/4}$, $0.4^{j\pi/4}$, $0.6^{j\pi/4}$, $0.8^{j\pi/4}$ and compare the SER performances to $\phi = 0$ ($\alpha_{1,2}$ is real) and $\phi = \pi/6$. For $\phi = \pi/4$, we show the SER vs S_2NR in Fig.: 7a) $|\alpha_{1,2}| = 0.2$, 7b) $|\alpha_{1,2}| = 0.4$, 7c) $|\alpha_{1,2}| = 0.6$, and 7d) $|\alpha_{1,2}| = 0.8$. Here, the conclusion to note is that there is a slight SER degradation for both Non-RSIC and RSIC scheme from $\phi = \pi/6$ to $\phi = \pi/4$. Interestingly the $\phi = \pi/6$ to $\phi = \pi/4$ phase shift has less SER effect compared to $\phi = 0$ to $\phi = \pi/6$ phase shift.

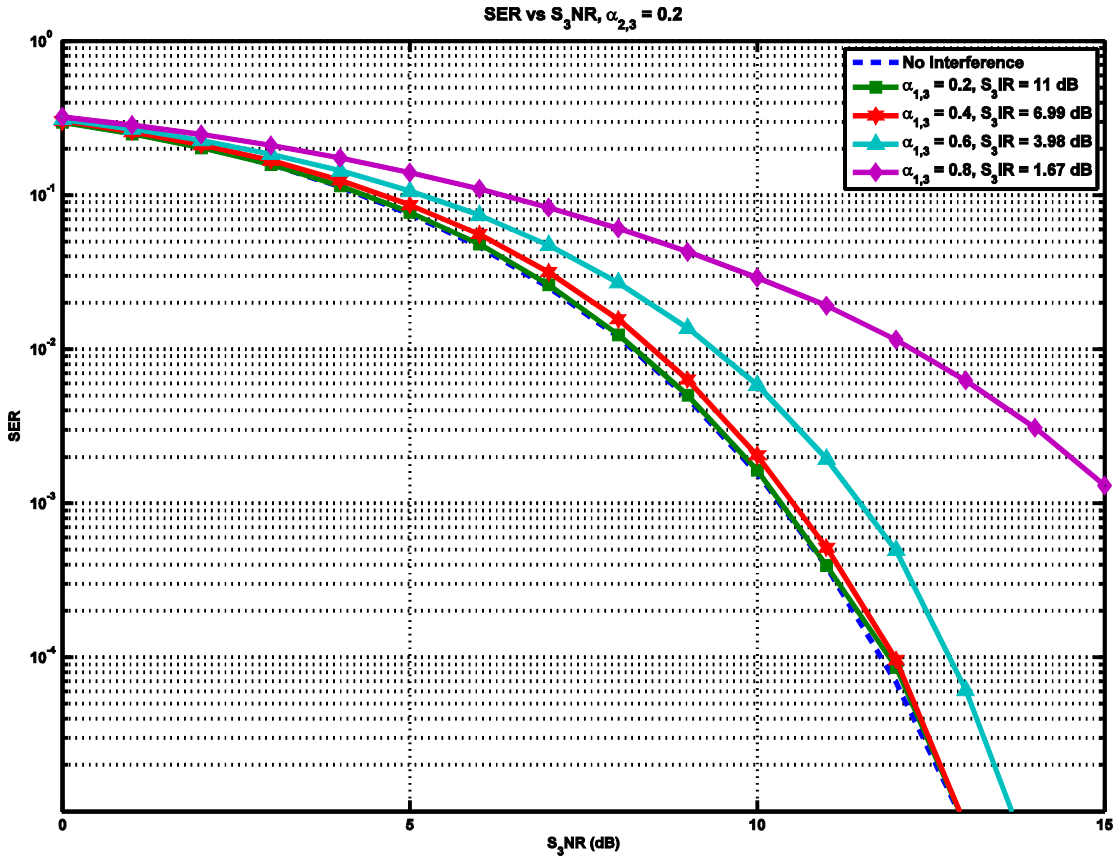

FIGURE 20. The RSIC performance curves of SER vs. S_3NR for demodulation of SoI s_3 in Rx_3 as a function of increasing $\alpha_{1,3}$ with $\alpha_{2,3} = 0.2$.

B. ESTIMATION RESULTS CORRESPONDING TO SER

Another useful set of results is the amplitude estimation corresponding to the set of SER results in Figs. 5, 6, and 7. The corresponding estimation results actually explain the remarkable RSIC SER performance. First we consider SER in Fig. 5 when phase offset is 0 ($\alpha_{1,2}$ is real). By plotting $\beta_{1,2}$ estimates along the actual amplitude value $\alpha_{1,2}$ as a function S_2NR in Fig. 8 and then showing how close the estimates approach the actual amplitude, a clear understanding is made of how S_2NR plays a role in parameter estimation. We can also plot the estimates as function of S_1NR in Rx2 which would be natural for estimation. However, we'll use S_2NR so we can conveniently see the correspondence to the SER results in Fig. 5 thereby illustrating the estimate's effect on SER which is not conveyed in the SER in Fig. 5. Notice that the estimates eventually approach the true parameters in Fig. 8a, 8b, and 8c at high S_2NR which explains why the SERs in Fig. 5a, 5b, and 5c eventually approach the interference-free SER. Estimates obviously improve with reduction of noise. However, with much higher interference level such as when $\alpha_{1,2} = 0.8$ in Fig. 8d, the estimate does not quite reach $\alpha_{1,2}$ (at least at S_2NR = 15 dB). This is the reason why the RSIC performance gain in Fig. 5d is the least among all $\alpha_{1,2}$ values. In other words, when the interference is large, the estimate is as not close to the actual parameter which makes the RSIC SER not as close to the interference-free SER. The corresponding estimates for SER results in Fig. 6 and Fig. 7 are shown in Fig. 9 and Fig. 10 respectively. Since $\alpha_{1,2}$ is complex with $\phi = \pi/6$ in Fig. 9 and $\phi = \pi/4$ in Fig. 10, both the magnitude estimate and phase estimate for $\beta_{1,2}$ are shown. If we compare the amplitude estimates from Fig. 8 ($\alpha_{1,2}$ is real) and the magnitude estimates in Fig. 9 ($\phi = \pi/6$), then we see that the phase shift makes the estimates worse. If we compare the magnitude estimates in Fig. 9 to the magnitude estimates in Fig. 10 ($\phi = \pi/4$), we see that the phase shift from $\pi/6$ to $\pi/4$ has less effect on the magnitude estimates compared to the phase shift from 0 to $\pi/6$. Now we can conclude that this is perhaps the reason why the SER differential between $\phi = 0$ to $\phi = \pi/6$ (Figs. 5 and 6) is worse than the SER differential between $\phi = \pi/6$ to $\phi = \pi/4$ (Figs. 6 and 7), a conclusion which would not have been apparent from Figs. 5, 6, and 7 alone. Interestingly, the phase estimates for $\phi = \pi/4$ are slightly better than for the case of $\phi = \pi/3$ which is a surprising result.

C. CRLB RESULTS CORRESPONDING TO SER AND ESTIMATION

Finally, an important comparison to perform in estimation is to compare the actual calculated variances to the CRLB. The variances of the $\beta_{1,2}$ estimates corresponding the Figs. 8, 9,

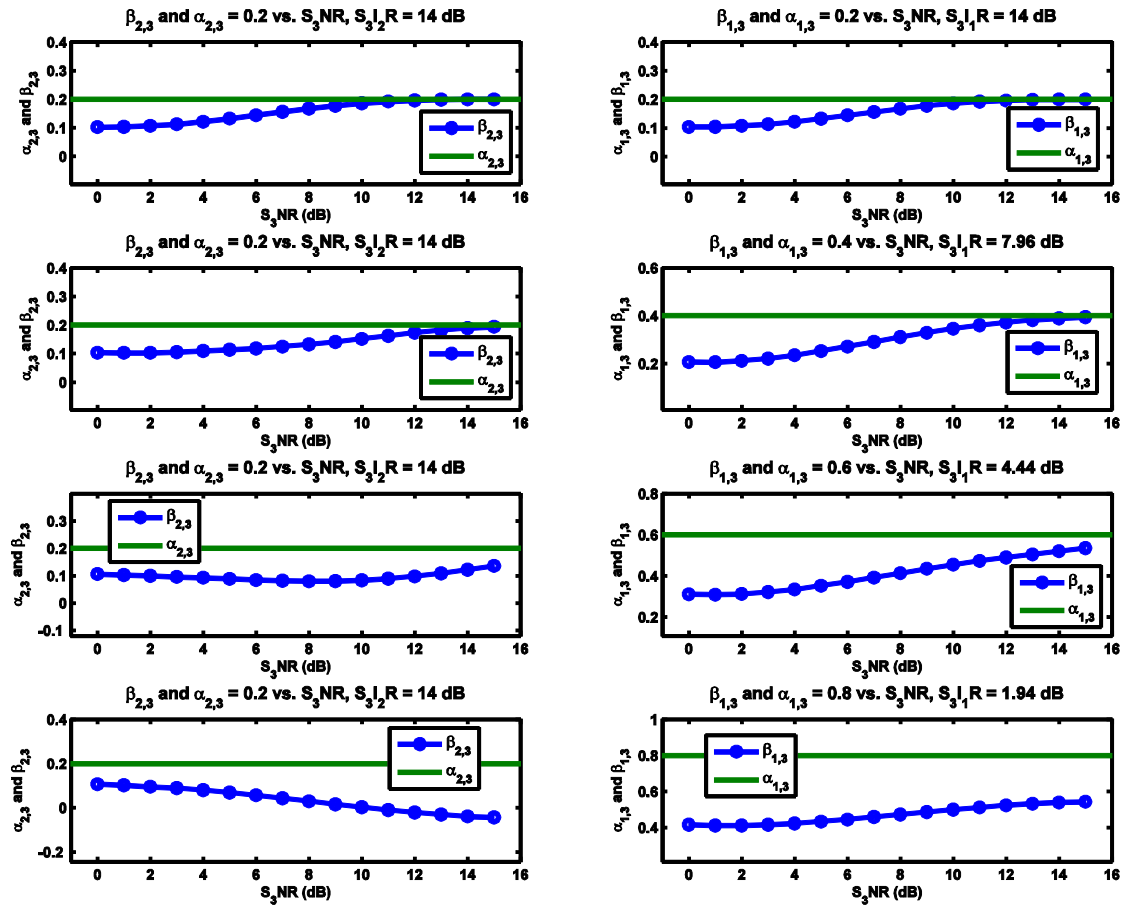

FIGURE 21. Receiver 3 estimates ($\beta_{2,3}$ and $\beta_{1,3}$) and actual parameters ($\alpha_{2,3}$ and $\alpha_{1,3}$) vs. S_3NR for $\alpha_{2,3} = 0.2$ which is paired with: $\alpha_{1,3} = 0.2$, 0.4, 0.6, and 0.8.

and 10 are calculated and compared to the variance calculated in (20) and/or (29), which interestingly can also be shown to be the CRLB if the system is without interference (i.e. only noise). While plotting the variance over S_2NR is insightful, in view of (20) we plot the variance as a function S_1NR (or equivalently interference-to-noise ratio, INR) in Rx2. We note that since we are using S_1NR, its range is not the same for each $\alpha_{1,2}$. Of course the corresponding S_2NR range in Figs. 11, 12, and 13 remains the same for each $\alpha_{1,2}$. The estimator variance vs. S_1NR in Fig. 11 corresponds to the SER with $\alpha_{1,2}$ being real (SER in Fig. 5 and amplitude estimate in Fig. 8). Note that for $\alpha_{1,2} = 0.2$, the estimator variance approaches the CRLB except for S_1NR values that are very low where it is widely known that the CRLB does not provide a good bound for such values. The fact that variance estimate approaches the CRLB for modest to high S_1NR is actually a good result since we recall that actual estimate carries with it some decoding errors i.e. the reference signal contains some demodulation errors (albeit small). As expected, the variance of $\beta_{1,2}$ decreases as S_1NR increases and the variance increases as $\alpha_{1,2}$ is increased. Once $\alpha_{1,2}$ starts to approach 1.0, even very high levels of S_1NR result in high variances of the estimate. The estimator variance vs. S_1NR curves in Fig. 12 and Fig. 13 correspond to the SER with $\alpha_{1,2}$ being complex with $\phi = \pi/6$ (SER in Fig. 6) to $\phi = \pi/4$ (SER in Fig. 7) respectively. The variance is actually the variance of the real part or the imaginary part of the estimator $\beta_{1,2}$ where simulations show that these variances are actually equal. From Fig. 12 ($\phi = \pi/6$), we note and now expect that the variance gets worse as $\alpha_{1,2}$ is increased and that the variance decreases as S_1NR increases. What is interesting is to compare variance vs S_1NR curves from Fig. 11 ($\alpha_{1,2}$ is real) and Fig. 12 ($\alpha_{1,2}$ is complex with $\phi = \pi/6$). Here we see that variance is worse for $\phi = \pi/6$ compared to $\phi = 0$. If we compare variance vs S_1NR curves from Fig. 12 ($\phi = \pi/6$) to Fig. 13 ($\phi = \pi/4$), we notice that the variance differential is lower than the variance differential from $\phi = 0$ to $\phi = \pi/6$.

IV. THREE-RECEIVER SYSTEM

We now expand the number of receivers to three which also corresponds to three SoIs. If we continue to use Fig. 1 as a reference, then a third signal is received by Rx_3 which is located in Sector C. Unfortunately, the received signal $\mathbf{y}_3$ contains two interfering signals. In Rx_3, the reference signals are contained in the IRM which is given by $\hat{\mathbf{S}} = [\hat{\mathbf{s}}_1 \ \hat{\mathbf{s}}_2]$. Recall that Rx_3 must first demodulate $\mathbf{y}_3$which may contain some errors due to the two interfering signals, which is given by $\tilde{\mathbf{s}}_3 = \text{dec}(\mathbf{y}_3)$

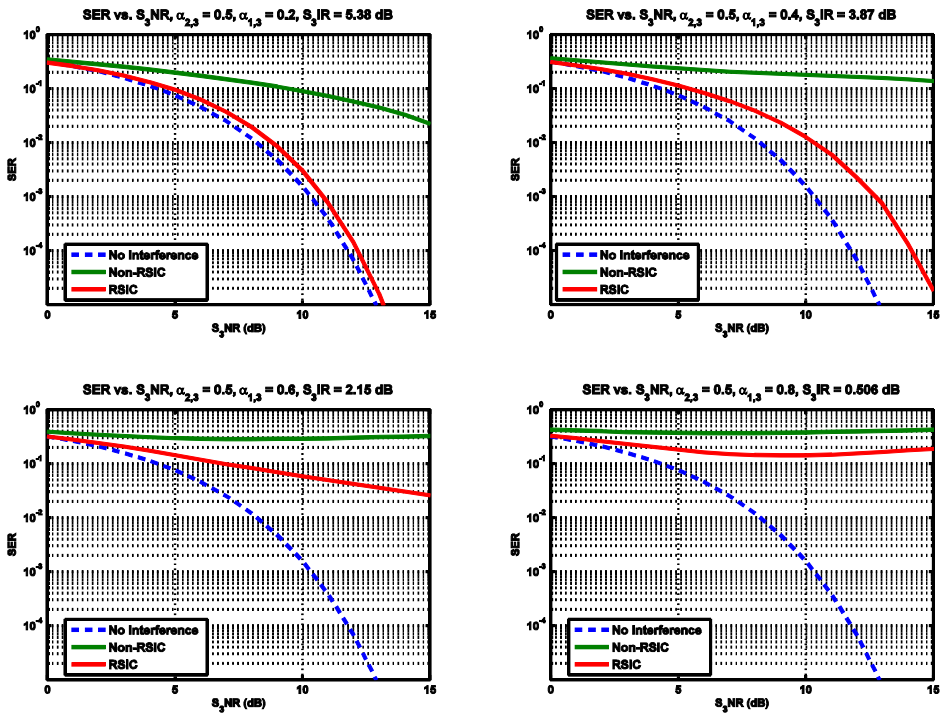

FIGURE 22. The performance curves of SER vs. S_3NR for demodulation of SoI s_3 in Rx_3 at different interference combinations when $\alpha_{2,3} = 0.5$: (a) $\alpha_{1,3} = 0.2$, $S_3IR = 5.38$ dB; (b) $\alpha_{1,3} = 0.4$, $S_3IR = 3.87$ dB; (c) $\alpha_{1,3} = 0.6$, $S_3IR = 2.15$ dB; (d) $\alpha_{1,3} = 0.8$, $S_3IR = 0.506$ dB.

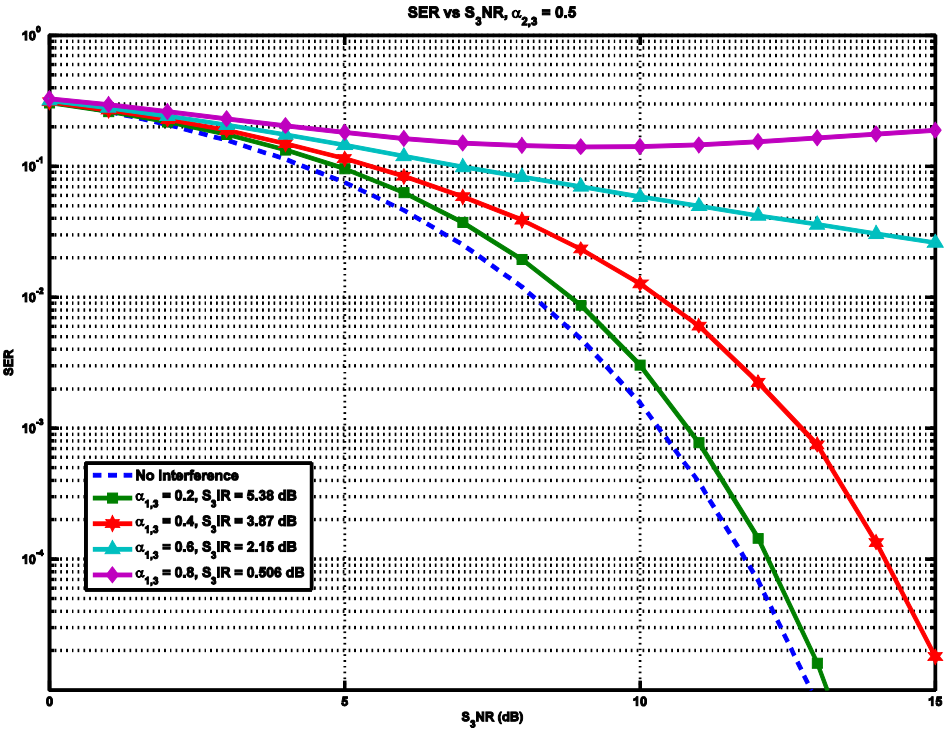

FIGURE 23. The RSIC performance curves of SER vs. S_3NR for demodulation of SoI s_3 in Rx_3 as a function of increasing $\alpha_{1,3}$ with $\alpha_{2,3} = 0.5$.

via MLD. In this case, the complex-valued estimate vector is given by $\boldsymbol{\beta}_3 = (\hat{\mathbf{S}}^H\hat{\mathbf{S}})^{-1}\hat{\mathbf{S}}^H(\mathbf{y}_3 - \tilde{\mathbf{s}}_3)$. Specifically, the estimate vector corresponding to the true $\boldsymbol{\alpha}_3 = [\alpha_{1,3}\ \ \alpha_{2,3}]^T$ vector is $\boldsymbol{\beta}_3 = [\beta_{1,3}\ \ \beta_{2,3}]^T$. Of course, if $\boldsymbol{\alpha}_3 = [\alpha_{1,3}\ \ \alpha_{2,3}]^T$ is all real then, $\boldsymbol{\beta}_3 = \left([\mathrm{Re}(\hat{\mathbf{S}}^H\hat{\mathbf{S}})]^{-1}\mathrm{Re}[\hat{\mathbf{S}}^H(\mathbf{y}_3 - \tilde{\mathbf{s}}_3)]\right)$. Utilizing amplitude estimates $\boldsymbol{\beta}_3 = [\beta_{1,3}\ \ \beta_{2,3}]^T$, we perform the RSIC demodulation of $\mathbf{s}_3$ as given by $\hat{\mathbf{s}}_3 = \mathrm{dec}(\mathbf{y}_3 - \beta_{1,3}\hat{\mathbf{s}}_1 - \beta_{2,3}\hat{\mathbf{s}}_2)$. Since our main interest

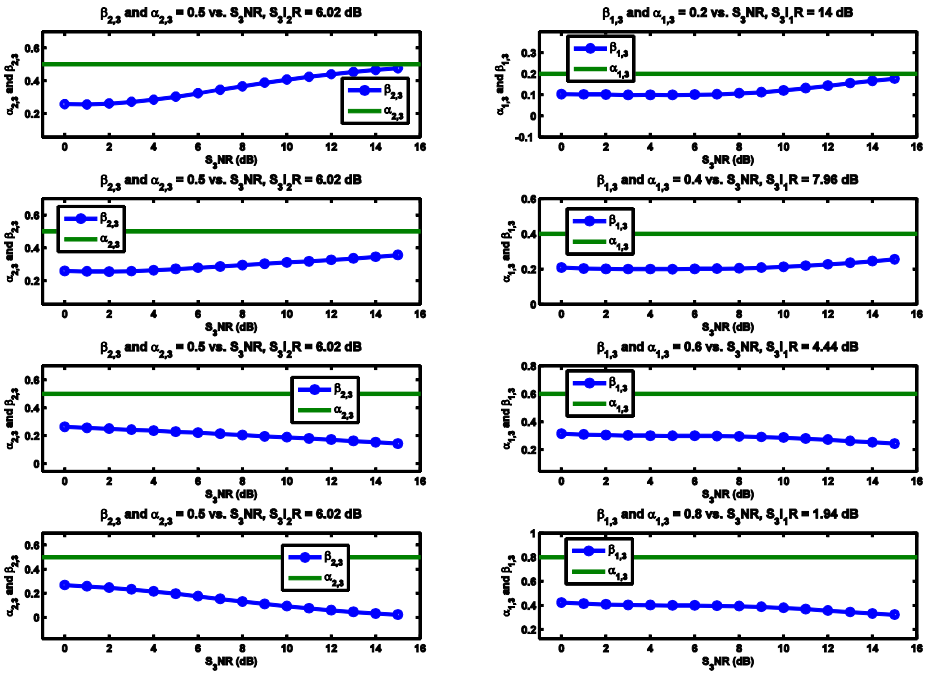

FIGURE 24. Receiver 3 estimates ($\beta_{2,3}$ and $\beta_{1,3}$) and actual parameters ($\alpha_{2,3}$ and $\alpha_{1,3}$) vs. S_3NR for $\alpha_{2,3} = 0.5$ which is paired with: $\alpha_{1,3} = 0.2$, 0.4, 0.6, and 0.8.

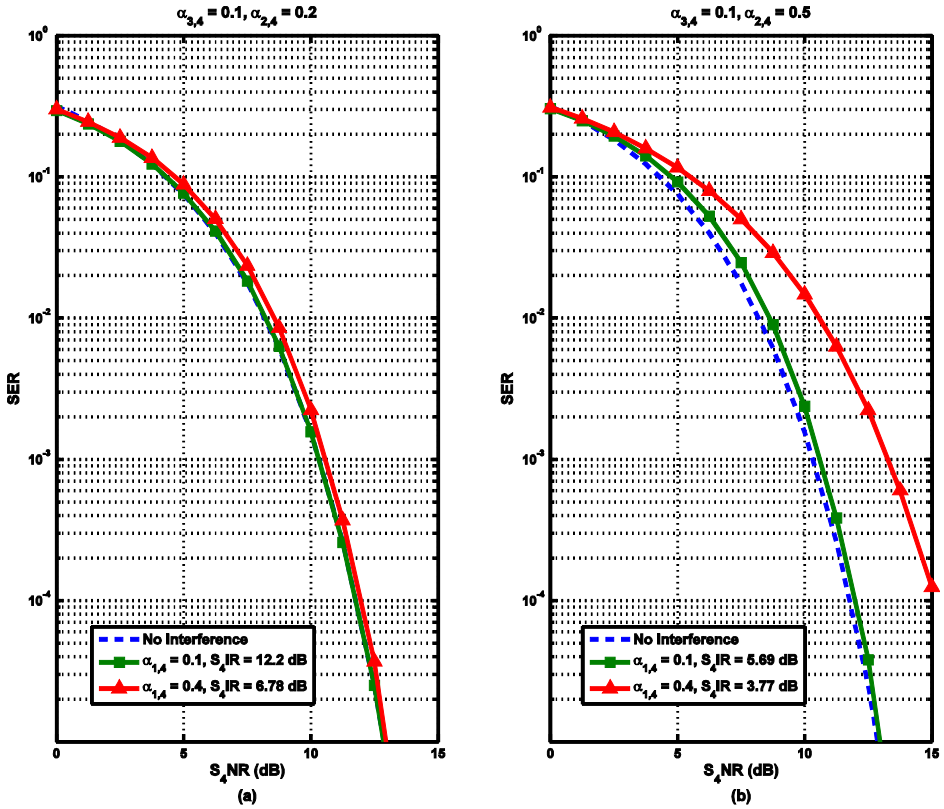

FIGURE 25. The RSIC SER vs. S_4NR for $\hat{s}_4$SoI demodulation at different interference combinations when $\alpha_{3,4} = 0.1$: (a) $\alpha_{2,4} = 0.2$; (b) $\alpha_{2,4} = 0.5$.

is SoI demodulation we will keep reporting in this section SER performance curves and the corresponding estimates versus true parameter (interference amplitude) results of which there'll be many due to the three receiver scenario. Thus in interest of brevity, we refrain from reporting any more variance vs CRLB comparison results since variance

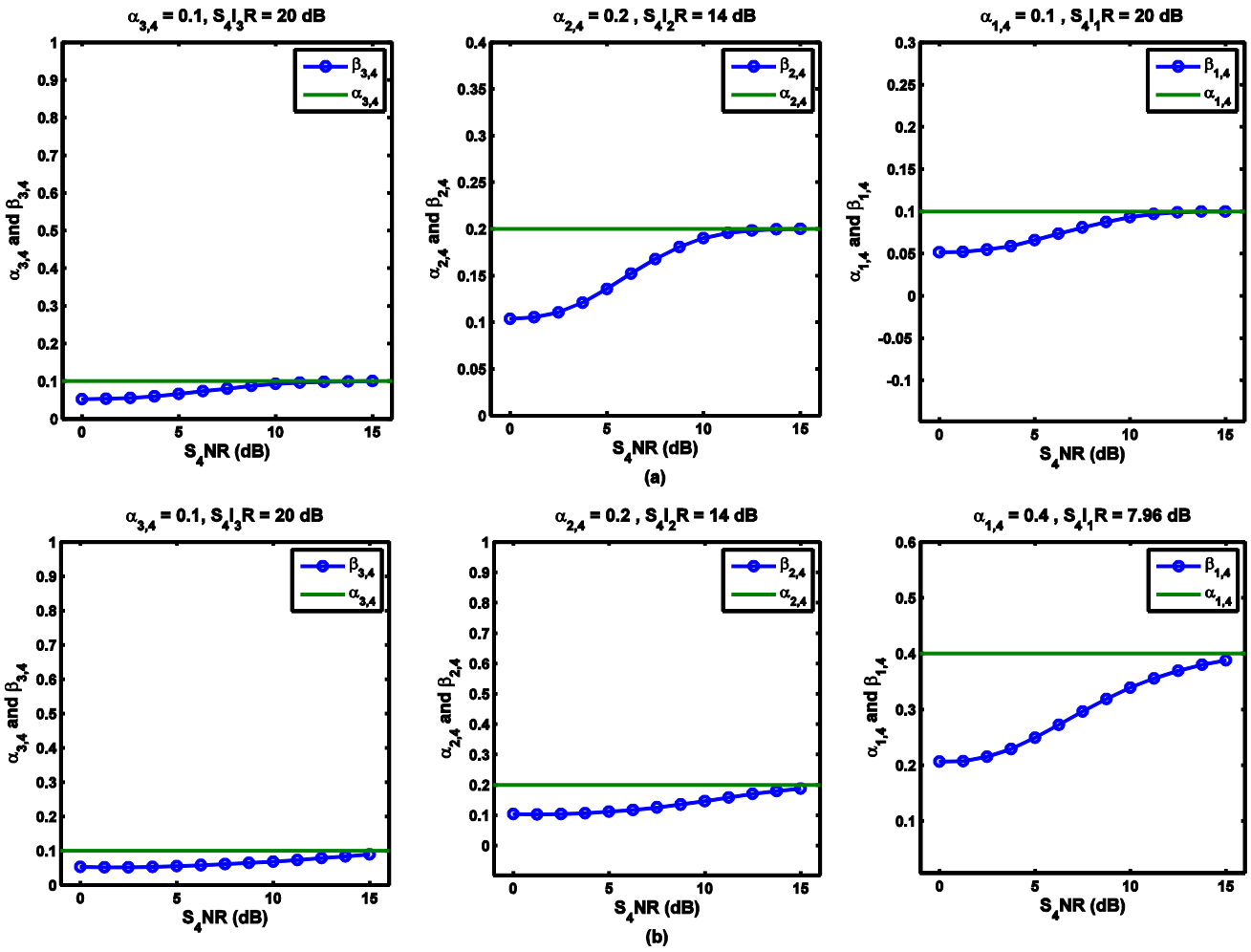

FIGURE 26. The plots of the actual parameters $\alpha_{3,4}$, $\alpha_{2,4}$, $\alpha_{1,4}$ and the estimators $\beta_{3,4}$, $\beta_{2,4}$, $\beta_{1,4}$ vs. S_4NR corresponding to: (a) $\alpha_{3,4} = 0.1$, $\alpha_{2,4} = 0.2$, $\alpha_{1,4} = 0.1$(S_4IR = 12.2 dB); and (b) $\alpha_{3,4} = 0.1$, $\alpha_{2,4} = 0.2$, $\alpha_{1,4} = 0.4$ (S_4IR = 6.78 dB).

calculations are straightforward with standard software computing tools.

1) ESTIMATION RESULTS: PARAMETERIZE S_3NR, VARY α_3

With two signals interfering the SoI $\mathbf{s}_3$, the signal-to-total-interference ratio is defined to be

$$\mathrm{S_3IR} \triangleq \frac{E_{\mathbf{s}_3}}{E_{\mathbf{s}_1} + E_{\mathbf{s}_2}} = \frac{\|\mathbf{s}_3\|^2}{\|\alpha_{1,3}\mathbf{s}_1\|^2 + \|\alpha_{2,3}\mathbf{s}_2\|^2} \tag{34}$$

which simplifies to

$$\mathrm{S_3IR} = \frac{1}{||\alpha_{1,3}||^2 + ||\alpha_{2,3}||^2}. \tag{35}$$

SIR due to individual signal interference is denoted as such (e.g. S_3I_2R and S_3I_1R). Since S_3IR includes both interferences (i.e. $\alpha_{1,3}$ and $\alpha_{2,3}$), there are numerous combinations that can be made in (34) or (35). Add the fact amplitudes are generally complex makes the number of combinations much larger (theoretically infinite in fact). Thus for the sake of brevity, we now just consider select combinations and consider $\boldsymbol{\alpha}_3 = [\alpha_{1,3}\ \alpha_{2,3}]^T$ is real (and positive) to reduce the number of practical results to be reported.

We investigate estimation by first holding Rx_3 SoI ($\mathbf{s}_3$) energy constant for various noise levels while varying interference amplitude values (varying S_3IR). For example, we can compare the estimates $\beta_{2,3}$ to $\alpha_{2,3}$ as a function of decreasing $\alpha_{2,3}$ (i.e. increasing S_3I_2R) for various noise levels (i.e. S_3NR levels). For $\alpha_{1,3} = 0.1$, 0.2, 0.5, and 0.8 we plot in Figs. 14a, 14c, 14e, and 14g $\beta_{2,3}$ estimates along with $\alpha_{2,3}$ as a function of increasing S_3I_2R for high S_3NR levels (10, 13, 20 dB). It is seen that as $\beta_{2,3}$ is varied at high S_3NR levels, $\beta_{2,3}$ estimates remain accurate with low $\alpha_{1,3}$ values such as 0.1 and 0.2, but heavily degrade at 0.5 and 0.8. This is not surprising since $\alpha_{1,3} = 0.5$ and $\alpha_{1,3} = 0.8$ result in high S_3IR despite $\alpha_{2,3}$ being low. In Figs. 14b, d, f, and h, $\beta_{2,3}$ estimates are plotted versus $\alpha_{2,3}$. The results corresponding to low S_3NR levels (0.97, 3.01, 6.99 dB) are shown in Fig. 15a-g where we see that estimates in a three-receiver system suffer worse compared to estimates corresponding to high S_3NR which is to be expected. Interestingly, for any $\alpha_{1,3}$ under large

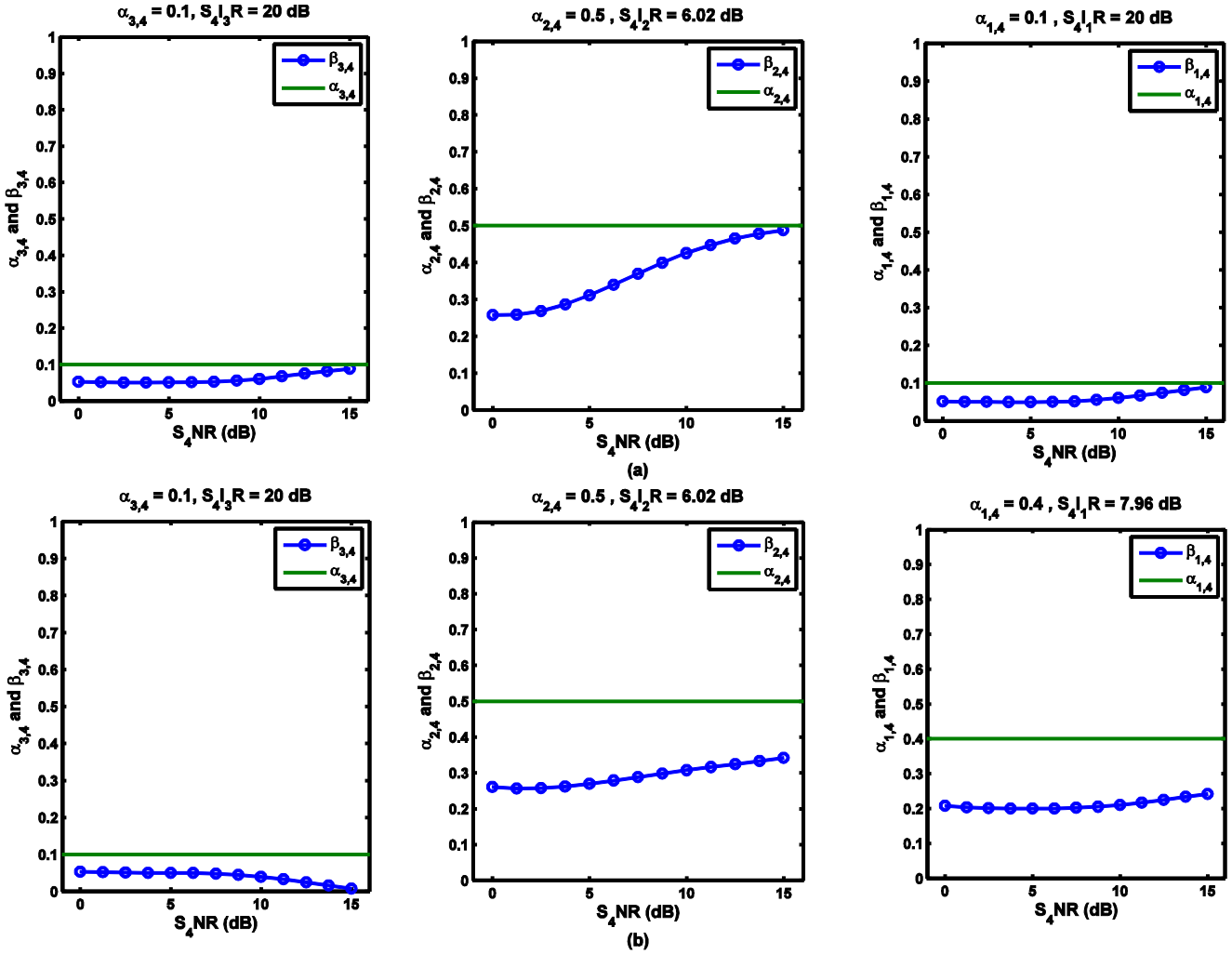

FIGURE 27. The plots of the actual parameters $\alpha_{3,4}$, $\alpha_{2,4}$, $\alpha_{1,4}$ and the estimators $\beta_{3,4}$, $\beta_{2,4}$, $\beta_{1,4}$ vs. S_4NR corresponding to: (a) $\alpha_{3,4} = 0.1$, $\alpha_{2,4} = 0.5$, $\alpha_{3,4} = 0.1$ (S_4IR = 5.69 dB); (b) $\alpha_{3,4} = 0.1$, $\alpha_{2,4} = 0.5$, $\alpha_{1,4} = 0.4$ (S_4IR = 3.77 dB).

amount of interference ($\alpha_{2,3}$ close to 1), the estimates for all S_3NR levels approaches 0.5 as seen in Figs. 14 and 15 where $\beta_{2,3}$ is plotted versus $\alpha_{2,3}$ which was also noted in the two-receiver system.

2) SER AND CORRESPONDING ESTIMATION RESULTS: PARAMETERIZE α_3, VARY S_3NR

Again the performance metric of utmost interest is SER (as a function of Rx_3 SoI SNR, i.e. S_3NR). Since we have two interference amplitudes ($\alpha_{2,3}$ and $\alpha_{1,3}$), we have to vary both with $\alpha_{1,3}$ taking the values 0.2, 0.4, 0.6 and 0.8 while we the parameter $\alpha_{2,3}$ changes to 0.1, 0.2, and 0.5 to illustrate their respective SERs as shown in Figures 16, 19, and 22. From these SERs we see the differing performances resulting from the multiple combinations of interference gain values.

When $\alpha_{2,3} = 0.1$ and $\alpha_{1,3} = 0.2$, 0.4, (Fig. 16a and 16b), we note that non-RSIC performance gets worse (compared to the two-receiver system from the previous section) but application of the RSIC moves the SER performances back closely to the interference-free SER. For the ($\alpha_{2,3} = 0.1$, $\alpha_{1,3} = 0.6$) pair, the Non-RSIC SER is heavily degraded and the corresponding RSIC SER becomes close to the interference-free SER for tremendous improvement. For the ($\alpha_{2,3} = 0.1$, $\alpha_{1,3} = 0.8$) pair, the Non-RSIC SER performance is so heavily degraded that it would be very difficult to successfully demodulate or retrieve the SoI. Fortunately, RSIC SER improves upon Non-RSIC and the SER retains the ''waterfall'' curve and remains acceptable even for this low value of S_3IR (1.87 dB)! For example, at 15dB S_3NR, the RSIC SER is over 3 decades better than the Non-RSIC. The SER performance for RSIC is summarized in Fig. 17 as a function of increasing $\alpha_{1,3}$ (with fixed $\alpha_{2,3} = 0.1$) such that the performance improvement for RSIC technique is appreciated.

Since $\alpha_{2,3} = 0.1$ and $\alpha_{1,3} = 0.2$, 0.4, 0.6, and 0.8, there are four pairs of interference estimates. The estimate curves are shown in Fig. 18. For $\alpha_{2,3} = 0.1$ and $\alpha_{1,3} = 0.2$ and 0.4, it is clear that the estimate pairs converge (almost con-

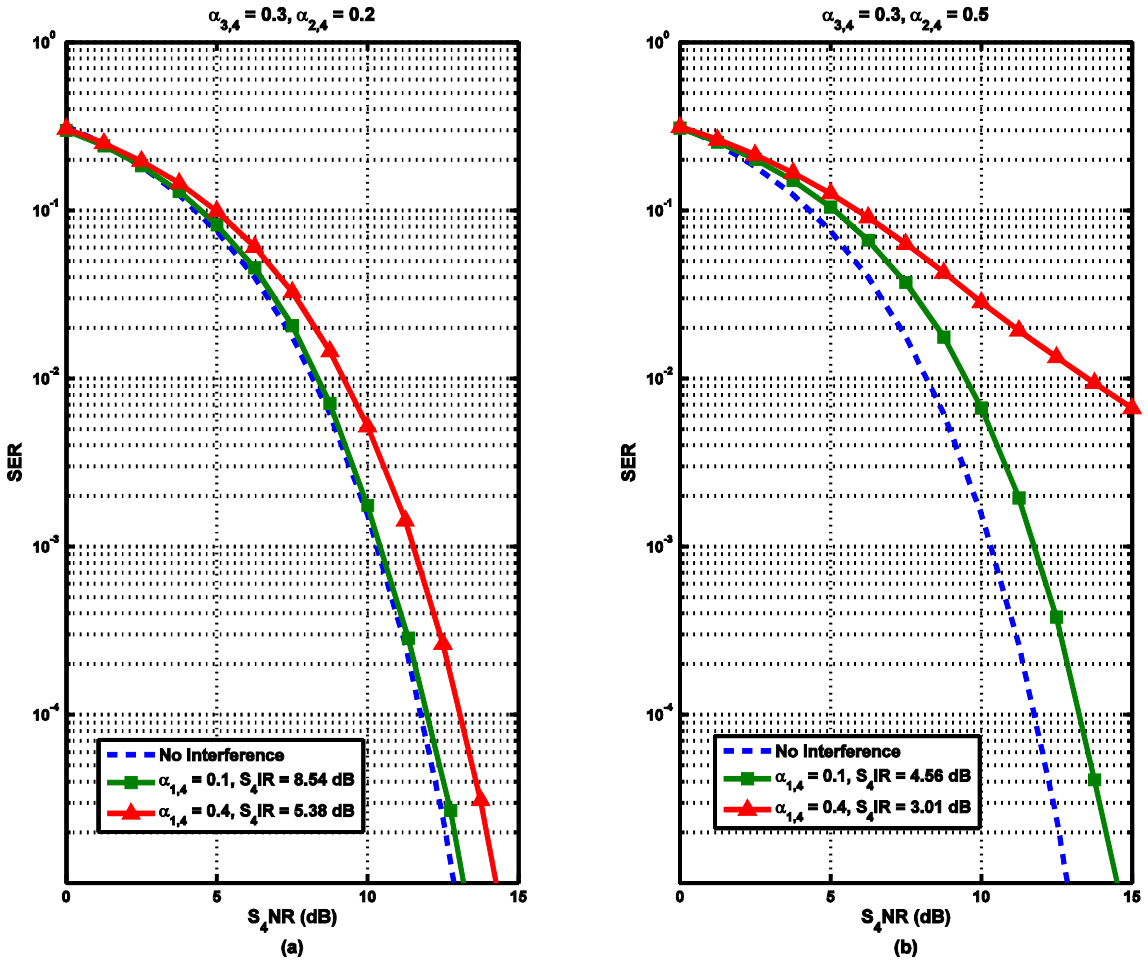

FIGURE 28. The RSIC SER vs. S_4NR for $\hat{s}_4$SoI demodulation at different interference combinations when $\alpha_{3,4} = 0.3$: (a) $\alpha_{2,4} = 0.2$; (b) $\alpha_{2,4} = 0.5$.

verges in the case of $\alpha_{1,3} = 0.6$) to the true parameters as S_3NR is increased. This is the reason why the RSIC performs well. Indeed, even for low S_3NR where the estimates are not close to the true parameters, RSIC also performs well. Notice however the case of ($\alpha_{2,3} = 0.1$, $\alpha_{1,3} = 0.8$) pair where estimate $\beta_{1,3}$ actually gets slightly worse as S_3NR is increased. The estimate $\beta_{1,3}$ is in a trajectory towards $\alpha_{1,3} = 0.8$ but does not reach it (at least not at S_3NR = 15 dB). This is the reason why the RSIC SER does not get as close to the interference-free SER for this pair. Nevertheless, its SER performance is a huge improvement from Non-RSIC.

With $\alpha_{2,3} = 0.2$ and $\alpha_{1,3} = 0.2$, 0.4, and 0.6 (Fig. 19a, 19b, and 19c), we note that non-RSIC performance gets worse (compared to the corresponding $\alpha_{2,3} = 0.1$ SER in Fig. 16a, 16b, and 16c) but yet again the application of the RSIC moves the SER performances back to the interference-free SER (for $\alpha_{1,3} = 0.2, 0.4$) or close to it (for $\alpha_{1,3} = 0.6$). For last pair, the Non-RSIC SER performance is heavily degraded as expected while RSIC SER still performs well enough in the sense that a waterfall-like curve is retained. At 15dB S_3NR, the RSIC SER is over 2 decades better than the Non-RSIC. The SER performance for RSIC is summarized in Fig. 20 as a function of increasing $\alpha_{1,3}$ (with fixed $\alpha_{2,3} = 0.2$). The four-pair estimates that correspond to the summarized SER results in Fig. 20 are shown in Fig. 21. For the first two-estimate pairs it is clear that the estimate pairs converge to the true parameters as S_3NR is increased. For third estimate pair, the estimate curves are in a trajectory towards but do not reach the parameter at S_3NR = 15 dB. It appears higher SNR is needed for these estimates to reach the true parameters. Again notice in the case of the last pair, the estimate $\beta_{2,3}$ gets even worse as S_3NR is increased compared to ($\alpha_{2,3} = 0.1$, $\alpha_{1,3} = 0.8$) pair. The estimate $\beta_{1,3}$ seems to improve but very slowly (to 0.54 at S_3NR = 15 dB where we recall that $\alpha_{1,3} = 0.8$).

With $\alpha_{2,3} = 0.5$ and $\alpha_{1,3} = 0.2$, and 0.4 (Fig. 22a and 22b), we note that non-RSIC performance gets worse (compared to the corresponding $\alpha_{2,3} = 0.2$ SER in Fig. 19a and Fig. 19b as expected). The SER (for $\alpha_{1,3} = 0.2$) is close to interference-free SER and the SER (for $\alpha_{1,3} = 0.4$) is respectable by retaining the waterfall curve. For the last two interference pairs, the Non-RSIC SER performances are truly unaccept-

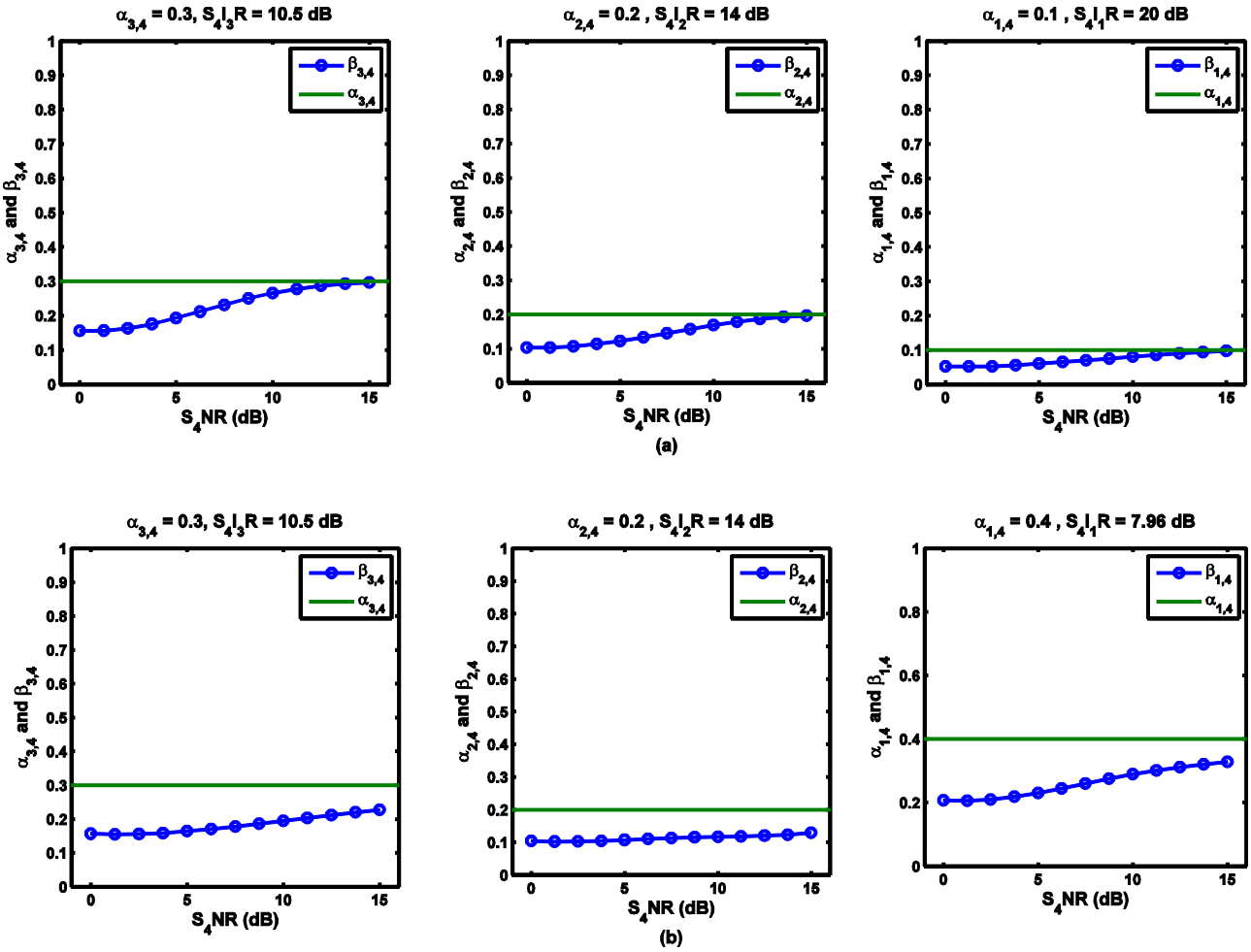

FIGURE 29. The plots of the actual parameters $\alpha_{3,4}$, $\alpha_{2,4}$, $\alpha_{1,4}$ and the estimators $\beta_{3,4}$, $\beta_{2,4}$, $\beta_{1,4}$ vs. different S_4NR values corresponding to: (a) $\alpha_{3,4} = 0.3$, $\alpha_{2,4} = 0.2$, $\alpha_{1,4} = 0.1$ (S_4IR = 8.54 dB); and (b) $\alpha_{3,4} = 0.3$, $\alpha_{2,4} = 0.2$, $\alpha_{1,4} = 0.4$ (S_4IR = 5.38 dB).

able (almost flat). For both pairs, RSIC SER is only slightly improved over Non-RSIC. This is because the S_3IR for the third pair is 2.15dB and the S_3IR for the fourth pair is 0.506 dB which are just too interference-limited. The SER performance for RSIC is summarized in Fig. 23. The four-pair estimates that correspond to the summarized SER results in Fig. 23 are shown in Fig. 24. For the first interference pair, it is clear that the estimates converge to the true parameters as S_3NR is increased which explains why the RSIC SER gets close the interference-free SER. For the second, the estimates are in a trajectory towards the true parameters as S_3NR is increased (but would require much higher S_3NR to do so). For the last two interference pairs, the estimates slightly get worse as S_3NR is increased. Rx_3 is just simply interference-limited for these two pairs of interference amplitudes which is why the RSIC can only improve so much in these cases.

In conclusion for the case of a three-receiver system, it is clear that RSIC performs very well in terms of SoI SER. From the interference combinations explored where the summarized SERs are shown in Figs. 17, 20, and 23, we can conclude that it performs well except when the aggregate SIR becomes very low.

V. FOUR-RECEIVER SYSTEM

Here we consider that a fourth receiver is added to the multi-receiver system. If we refer to Fig. 1 the fourth receiver takes a position somewhere in Sector D. The received signal $\mathbf{y}_4$ contains three interfering signals signals: $\mathbf{s}_1$, $\mathbf{s}_2$ and $\mathbf{s}_3$ each of which has its own interference amplitude given by $\boldsymbol{\alpha}_4 = [\alpha_{1,4} \ \alpha_{2,4} \ \alpha_{3,4}]^T$. Recall that in order to estimate these amplitudes we need an initial guess for $\mathbf{s}_4$ in Rx_4 which is given by $\tilde{\mathbf{s}}_4 = \text{dec}(\mathbf{y}_4)$. Since we have 3 interfering signals, the SER is potentially worse than the three-receiver system. The complex-valued estimate vector $\boldsymbol{\beta}_4 = [\beta_{1,4} \ \beta_{2,4} \ \beta_{3,4}]^T$ is given by $\boldsymbol{\beta}_4 = (\hat{\mathbf{S}}^H \hat{\mathbf{S}})^{-1} \hat{\mathbf{S}}^H \left(\mathbf{y}_4 - \tilde{\mathbf{s}}_4\right)$ where the IRM is now given by $\hat{\mathbf{S}} = [\hat{\mathbf{s}}_1 \ \hat{\mathbf{s}}_2 \ \hat{\mathbf{s}}_3]$. If the interference amplitudes in $\boldsymbol{\alpha}_4 = [\alpha_{1,4} \ \alpha_{2,4} \ \alpha_{3,4}]^T$ are real then the estimate vector β_4 is given by $\beta_4 = \left([\text{Re}(\hat{\mathbf{S}}^H \hat{\mathbf{S}})]^{-1} \text{Re}[\hat{\mathbf{S}}^H (\mathbf{y}_4 - \tilde{\mathbf{s}}_4)]\right)$. Rx_4 SoI is then given by $\hat{\mathbf{s}}_4 = \text{dec}(\mathbf{y}_4 - \beta_{1,4}\hat{\mathbf{s}}_1 - \beta_{2,4}\hat{\mathbf{s}}_2 - \beta_{3,4}\hat{\mathbf{s}}_3)$.

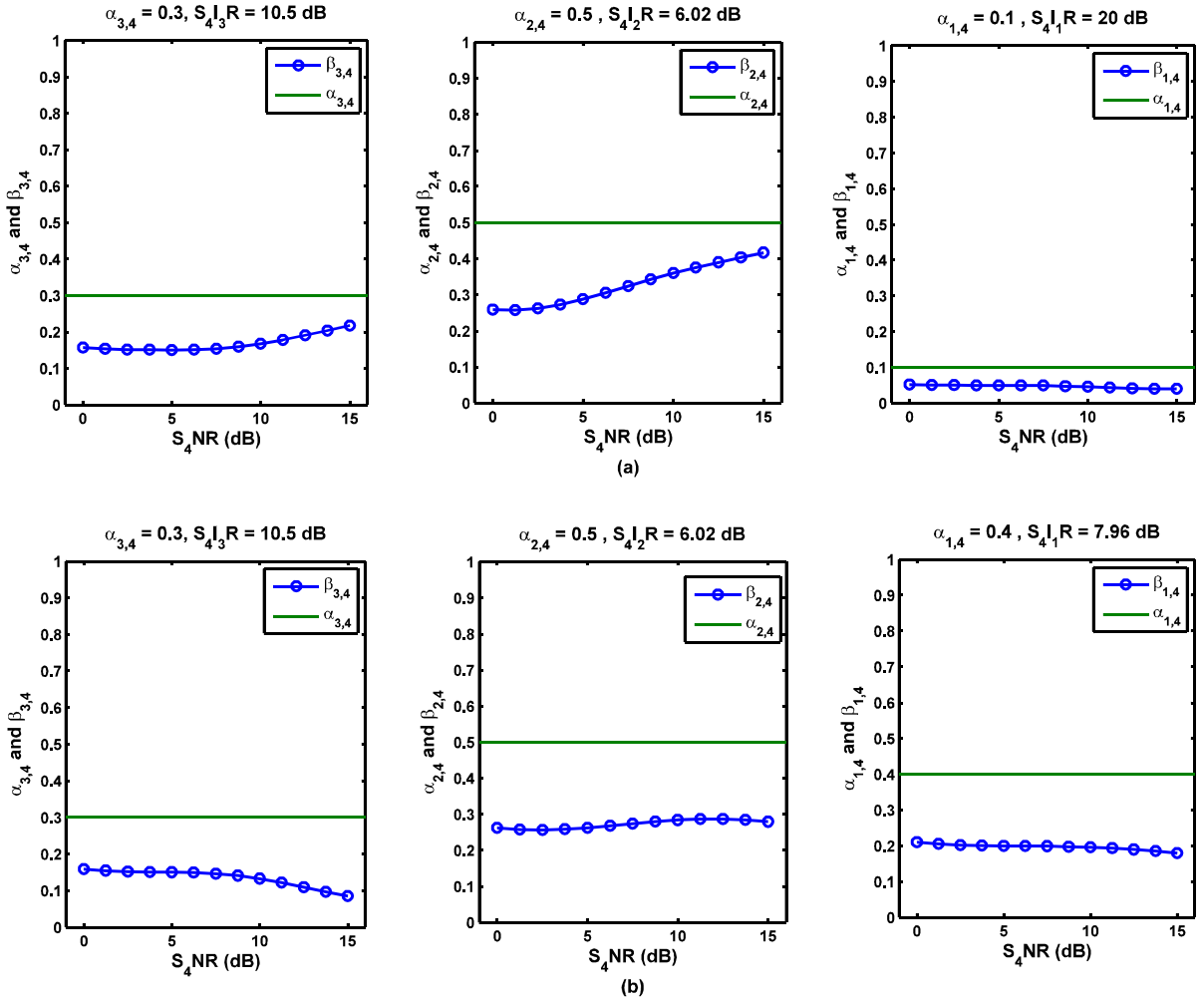

FIGURE 30. The plots of the actual parameters $\alpha_{3,4}$, $\alpha_{2,4}$, $\alpha_{1,4}$ and the estimators $\beta_{3,4}$, $\beta_{2,4}$, $\beta_{1,4}$ vs. different S_4NR values corresponding to: (a) $\alpha_{3,4} = 0.3$, $\alpha_{2,4} = 0.5$, $\alpha_{1,4} = 0.1$ (S_4IR = 4.56 dB); and (b) $\alpha_{3,4} = 0.3$, $\alpha_{2,4} = 0.5$, $\alpha_{1,4} = 0.4$ (S_4IR = 3.01 dB).

The total SIR in Rx_4 is given by

$$S_4\text{IR} \triangleq \frac{E_{s_4}}{E_{s_1} + E_{s_2} + E_{s_3}} = \frac{\|s_4\|^2}{\|\alpha_{1,4}s_1\|^2 + \|\alpha_{2,4}s_2\|^2 + \|\alpha_{3,4}s_3\|^2} \quad (36)$$

which simplifies to

$$S_4\text{IR} = \frac{1}{||\alpha_{1,4}||^2 + ||\alpha_{2,4}||^2 + ||\alpha_{3,4}||^2}. \quad (37)$$

Now that S_4IR includes three interferences, there are even more SIR combinations in (37) compared to the three-receiver case. Again for the sake of brevity, we now just consider select combinations and consider the amplitudes to be real (and positive) to reduce the number of example results. Moreover, we limit our report on RSIC SERs and their corresponding estimation results. We also now refrain from reporting Non-RSIC (MLD without any interference cancellation) since it performs terribly in the four-receiver case. This is true for some cases even when the SNR is large and SIR is modest.

1) INTERFERENCE COMBINATIONS $\alpha_{3,4} = 0.1$ $\alpha_{2,4} = 0.2, 0.5$, $\alpha_{1,4} = 0.1, 0.4$:

To generate SER and estimation results for RSIC let us consider the following cases: $\alpha_{3,4} = 0.1$, $\alpha_{2,4} = 0.2, 0.5$, $\alpha_{1,4} = 0.1, 0.4$. This results in four interference amplitude combinations that yield S_4IR of 12.2, 6.78, 5.69, and 3.77 dB. The RSIC SERs corresponding to these 4 interference amplitude combinations are shown in Fig. 25. Notice that the interference combinations corresponding to S_4IR of 12.2, 6.78, and 5.69 dB result in SERs that approach the interference-free SER. The RSIC SER corresponding to a total SIR = 3.77 dB does not approach the interference-free SER but retains the waterfall curve. We note that the SERs corresponding to S_4IR = 6.78 and 5.69 dB closely approach the interference-free SER at high SNR. However at medium SNR, the SERs are close but there seems to be discernable small gaps to the interference-free SER. These "small" gaps were actually present in a few of the 3-receiver RSIC SER results from previous section but were not explored upon. To explain this interesting phenomenon, we look at the

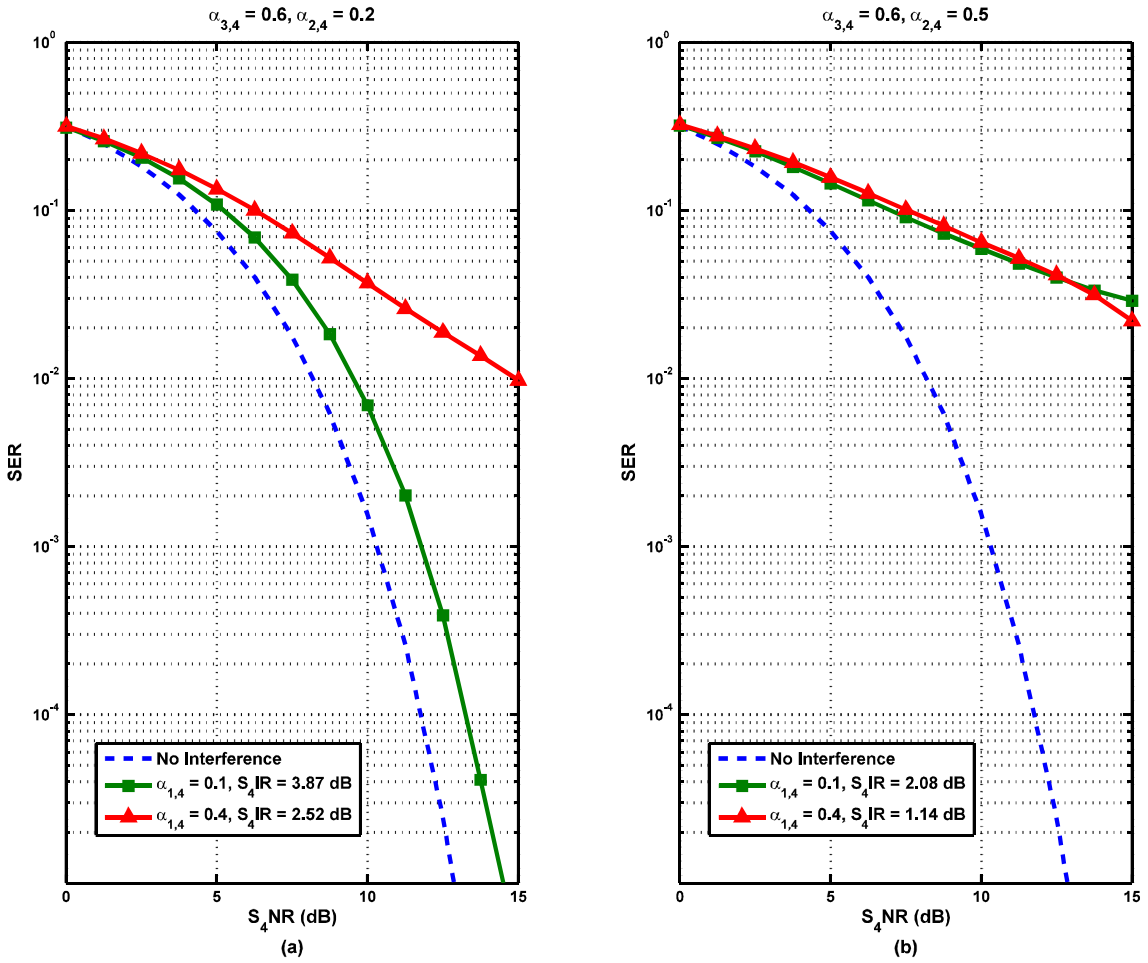

FIGURE 31. The RSIC SER vs. S_4NR for $\hat{s}_4$ SoI demodulation at different interference combinations when $\alpha_{3,4} = 0.6$: (a) $\alpha_{2,4} = 0.2$; (b) $\alpha_{2,4} = 0.5$.

amplitude estimates corresponding to these SERs. The plots of the estimators $\beta_{3,4}, \beta_{2,4}, \beta_{1,4}$ (along with the actual parameters $\alpha_{3,4}, \alpha_{2,4}, \alpha_{1,4}$) vs. different S_4NR values corresponding to S_4IR = 12.2 dB and S_4IR = 6.78 dB are shown in Fig. 26. For S_4IR = 5.69 dB and S_4IR = 3.77 dB, the plots are shown in Fig. 27. Each estimate curve is also labeled with the corresponding individual SIR. For example, the estimate curve located far-right of Fig. 26a for $\alpha_{1,4} = 0.1$ has a label $S_4I_1R = 20$ dB but recall that the aggregate S_4IR is 12.2 dB. For S_4IR of 6.78, and 5.69 dB where the SER "gaps" exist, the estimates start to converge to the actual parameters at high S_4NR but not at medium S_4NR. The fact that the estimates have not converged to the actual parameters is the reason why there are small SER gaps between RSIC SER and interference-free SER. Nevertheless, it is still impressive that the RSIC is able to incredibly improve upon the Non-RSIC SER performance despite the estimates not being close to the actual amplitude parameters at medium SNR. Interestingly, at low SNR the accuracy of the estimates does not affect the SER as evidenced in most of the SER plots even when the SIR is low. This is because at low SNR, the actual receiver noise starts to become more dominant compared to the interferers. This is why the small SER gaps (which we now know happens when the estimates do not converge to the actual true parameters) only appear in the medium SNR area. Such conclusions can't be made without running various parameterized simulations.

2) INTERFERENCE COMBINATIONS $\alpha_{3,4} = 0.3$, $\alpha_{2,4} = 0.2, 0.5$, $\alpha_{1,4} = 0.1, 0.4$:

To generate different SIR values, we now hold to $\alpha_{3,4}$ constant and vary the other two interference amplitudes. Specifically we look at the set: $\alpha_{3,4} = 0.3$, $\alpha_{2,4} = 0.2, 0.5$, $\alpha_{1,4} = 0.1, 0.4$ which yields four S_4IRs of 8.54, 5.38, 4.56, and 3.01 dB. The corresponding RSIC SERs are shown in Fig. 28. Here notice that the SER corresponding to S_4IR of 8.54 dB is the only one that approaches the interference-free SER. For S_4IR 5.38 and 4.56 dB, the SERs are still effective in the sense they still have the shape of the waterfall curve. For S4IR = 3.01 dB, the SER improves very slowly as a function of increasing SNR and is therefore not as effective. The plots of the actual parameters $\alpha_{3,4}$, $\alpha_{2,4}$, $\alpha_{1,4}$ and the estimators $\beta_{3,4}$, $\beta_{2,4}$, $\beta_{1,4}$ vs. S_4NR corresponding to

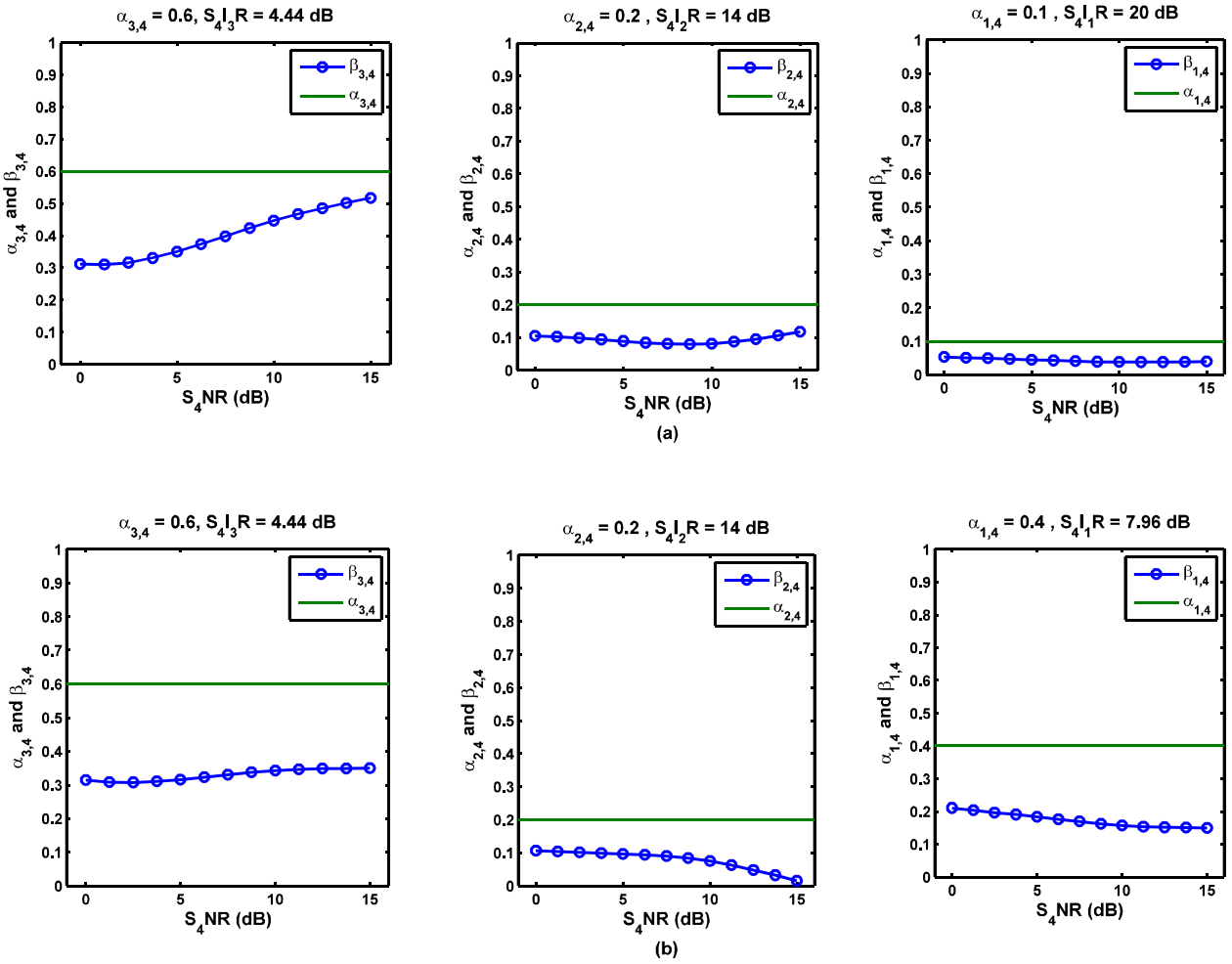

FIGURE 32. The plots of the actual parameters $\alpha_{3,4}$, $\alpha_{2,4}$, $\alpha_{1,4}$ and the estimators $\beta_{3,4}$, $\beta_{2,4}$, $\beta_{1,4}$ vs. S_4NR for multiple simulations of y_4: (a) S_4IR = 3.87 dB; (b) S_4IR = 2.52 dB.

$\alpha_{3,4} = 0.3$, $\alpha_{2,4} = 0.2$, $\alpha_{1,4} = 0.1$ (S_4IR = 8.54 dB), $\alpha_{3,4} = 0.3$, $\alpha_{2,4} = 0.2$, $\alpha_{1,4} = 0.4$ (S_4IR = 5.38 dB), $\alpha_{1,4} = 0.3$, $\alpha_{2,4} = 0.5$, $\alpha_{3,4} = 0.1$ (S_4IR = 4.56 dB), and $\alpha_{1,4} = 0.3$, $\alpha_{2,4} = 0.5$, $\alpha_{3,4} = 0.4$ (S_4IR = 3.01 dB) are shown in Fig. 29 and Fig. 30. It is clear that only the estimates corresponding to S_4IR = 8.54 dB approach the actual parameter values which explains why the RSIC SER corresponding to this SIR approaches the interference-free SER. Notice that at S_4IR = 5.38 dB the RSIC SER is very close but it does not approach the interference-free SER. At this SIR, the three estimates improve as a function of increasing SNR (although do not converge to the actual parameter values at SNR = 15dB). The set of estimates for S_4IR = 4.56 dB is a good example where there is a mixture of estimation performance which (9) does not easily convey. Two of the estimates improve as SNR is increased while the estimate $\beta_{1,4}$ actually gets worse as SNR is increased. Nevertheless just like the SER corresponding to S_4IR = 5.38 dB, the SER corresponding S_4IR = 4.56 dB retains its waterfall curve which is still deemed effective. The estimate corresponding S_4IR = 3.01 dB actually gets worse as function of increasing SNR. Although the SER improves (over Non-RSIC), it is deemed less effective.

3) INTERFERENCE COMBINATIONS $\alpha_{3,4} = 0.6$, $\alpha_{2,4} = 0.2, 0.5$, $\alpha_{1,4} = 0.1, 0.4$:

Our goal in this section is to generate much higher SIR values to see where RSIC becomes less effective in terms of aggregate SIR, so we increase $\alpha_{3,4}$ to 0.6 (from the previous interference combination). Thus, we have $\alpha_{3,4} = 0.6$, $\alpha_{2,4} = 0.2, 0.5$, $\alpha_{1,4} = 0.1, 0.4$ which yields four very low S_4IRs of 3.87, 2.52, 2.08, and 1.14 dB. The corresponding RSIC SERs are shown in Fig. 31. With the SIR being very low, none of the SERs approaches the interference-free SER. In fact, only the SER corresponding to 3.87 dB is deemed effective. The SERs corresponding to the last 3 SIRs do not retain the shape of the waterfall curve and are deemed less effective. The plots of the actual gain parameters $\alpha_{3,4}$, $\alpha_{2,4}$, $\alpha_{1,4}$ and the estimators $\beta_{3,4}$, $\beta_{2,4}$, $\beta_{1,4}$ vs. S_4NR corresponding to S_4IR = 3.87 dB, S_4IR = 2.52 dB, S_4IR = 2.08 dB, and S_4IR = 1.14 dB are shown in Fig. 32 and Fig. 33. We have a variety of interesting results that we

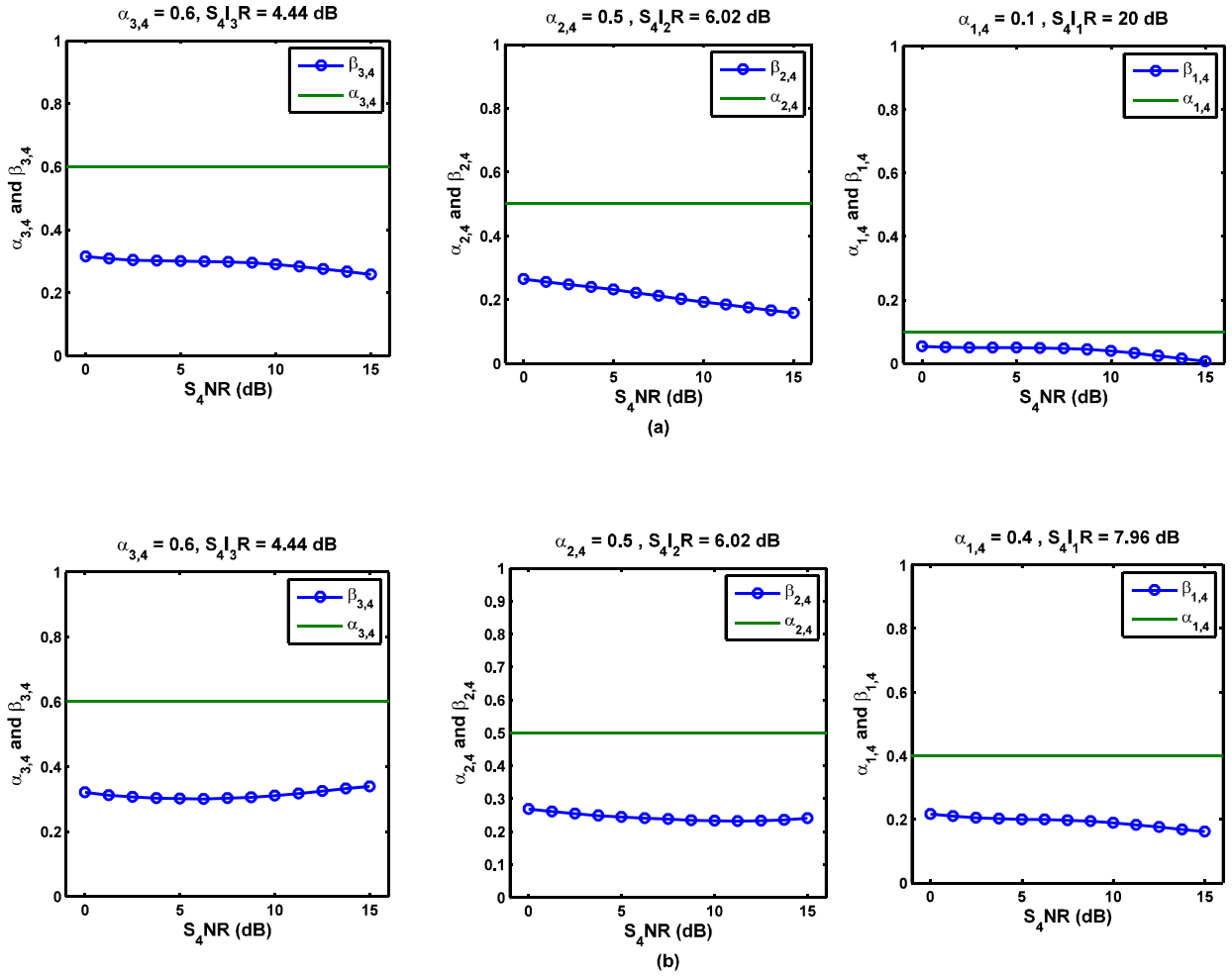

FIGURE 33. The plots of the actual parameters $\alpha_{3,4}$, $\alpha_{2,4}$, $\alpha_{1,4}$ and the estimators $\beta_{3,4}$, $\beta_{2,4}$, $\beta_{1,4}$ vs. S_4NR for multiple simulations of y_4: (a) S_4IR = 2.08 dB; (b) S_4IR = 1.14 dB.

can discuss as to how the individual estimates behave. But we only look at the estimate set belonging to S_4IR = 3.87 dB since we already know that the rest of the SIRs result in less effective SERs. Even for S_4IR = 3.87 dB, the three estimates behave differently: the estimate $\beta_{3,4}$ strictly improves as a function of increasing SNR, the estimate $\beta_{2,4}$ actually gets worse in the medium SNR range but seems to improve at high SNR, and $\beta_{1,4}$ gets worse as a function of SNR.

It may be tempting to conclude that the aggregate SIR given a number of interferers is the only metric that dictate the RSIC SER (or regardless of the number of interferers for that matter). However, this is not the case. For example, if we look at the SER corresponding to RSIC SER for $\alpha_{3,4} = 0.3$, $\alpha_{2,4} = 0.5$, $\alpha_{1,4} = 0.1$ (S_4IR = 4.56 dB) in Fig. 28b we note that this SER is almost equal to the RSIC SER for $\alpha_{3,4} = 0.6$, $\alpha_{2,4} = 0.2$, $\alpha_{1,4} = 0.1$ (S_4IR = 3.87 dB) in Fig. 31a despite the fact that the latter has lower aggregate SIR than the former. This is a surprising result that is not apparent in any of the equations presented in this work. The key is to look at the quality of the estimates. Better set of estimates (a set where the estimates which tend to converge to the true interference amplitudes) generally results in better RSIC SER.

VI CONCLUSION

In this paper, we introduced and developed a novel technique of retrieving (i.e. demodulating) signals of interest (SoI) with the use of multiple receivers that are physically far apart for the purposes of signal collection applications which can extend to SIGINT, ELINT and/or COMINT applications. We call the technique RSIC (reference-based signal interference cancellation) and it involves the combination of strategic receiver location and a clever mixture of signal processing techniques. Each receiver is assigned to capture a single SoI. In other words, other signals act as interference to that SoI. The scheme involves placing the receivers in locations of opportunities where an initial receiver is placed where only one SoI is present. This SoI (which is called a reference signal) is passed on to the second receiver which

tries to collect a different SoI in which the received signal is interfered by the initial SoI. So, the second receiver uses the reference forwarded by the first receiver for cancellation (subtraction). The problem however is that the second receiver does not know its amplitude and thus subtraction cannot easily be performed. Thus, it is proposed to be estimated. Unfortunately, the initial LSE estimation requires the knowledge of the second SoI which is the very signal the second receiver is trying to demodulate thereby yielding an interesting "Catch-22" problem. To solve this problem, we proposed to demodulate the received signal (despite being filled with interference) and use that as "initial guess" for estimation of the interference amplitude prior to subtraction. Once the estimate is available, we perform the subtraction, and we re-demodulate the resulting difference. This technique worked amazingly well! The technique is easily extended to multiple SoIs with the use of multiple receivers. While the technique is useful for various signals, the ubiquity of communication signals due to wireless applications prompted us to use a widely known signal modulation (QPSK) in our example simulations. Thus, we monitored symbol error rate as our performance metric along with the estimates and variance comparison to the CRLB. We showed various interference combinations where the Non-RSIC (i.e. using only maximum likelihood detection) simply did not work well and resulted in heavily degraded SER. When RSIC was applied, the SER actually approached the interference-free SER even for modest SIR. While the RSIC SER performance was tied to aggregate SIR, it was actually the quality of the estimates that dictated how well RSIC performed.

APPENDIX

A. DIFFERENTIATION FOR LSE

First, we expand (5) such that

$$\begin{aligned} J(\boldsymbol{\alpha}_n) &= (\mathbf{y}_n - \mathbf{s}_n - \mathbf{S}\boldsymbol{\alpha}_n)^H(\mathbf{y}_n - \mathbf{s}_n - \mathbf{S}\boldsymbol{\alpha}_n) \\ &= (\mathbf{y}_n^H - \mathbf{s}_n^H - \boldsymbol{\alpha}_n^H\mathbf{S}^H)(\mathbf{y}_n - \mathbf{s}_n - \mathbf{S}\boldsymbol{\alpha}_n) \\ &= \mathbf{y}_n^H\mathbf{y}_n - \mathbf{y}_n^H\mathbf{s}_n - \mathbf{y}_n^H\mathbf{S}\boldsymbol{\alpha}_n - \mathbf{s}_n^H\mathbf{y}_n + \mathbf{s}_n^H\mathbf{s}_n + \mathbf{s}_n^H\mathbf{S}\boldsymbol{\alpha}_n \\ &\quad -\boldsymbol{\alpha}_n^H\mathbf{S}^H\mathbf{y}_n + \boldsymbol{\alpha}_n^H\mathbf{S}^H\mathbf{s}_n + \boldsymbol{\alpha}_n^H\mathbf{S}^H\mathbf{S}\boldsymbol{\alpha}_n. \end{aligned} \tag{A1}$$

The derivative of $J(\boldsymbol{\alpha}_n)$ with respect to the $(n-1)\times 1$ complex vector $\boldsymbol{\alpha}_n$ can be evaluated using the identity $\partial\mathbf{b}^H\boldsymbol{\theta}/\partial\boldsymbol{\theta} = \mathbf{b}^*$ where $\mathbf{b}$ and $\boldsymbol{\theta}$ are both $(n-1)\times 1$ complex vectors [14]. Taking the derivative of (A1) yields

$$\begin{aligned} \frac{\partial J(\boldsymbol{\alpha}_n)}{\partial\boldsymbol{\alpha}_n} &= -\frac{\partial}{\partial\boldsymbol{\alpha}_n}\left[\left(\mathbf{S}^H\mathbf{y}_n\right)^H\boldsymbol{\alpha}_n\right] \\ &\quad +\frac{\partial}{\partial\boldsymbol{\alpha}_n}\left[\left(\mathbf{S}^H\mathbf{s}_n\right)^H\boldsymbol{\alpha}_n\right] + \frac{\partial}{\partial\boldsymbol{\alpha}_n}\left[\boldsymbol{\alpha}_n^H\mathbf{S}^H\mathbf{S}\boldsymbol{\alpha}_n\right] \\ &= -\left(S^H\mathbf{y}_n\right)^* + \left(\mathbf{S}^H\mathbf{s}_n\right)^* + \left(\mathbf{S}^H\mathbf{S}\boldsymbol{\alpha}_n\right)^* \end{aligned} \tag{A2}$$

Setting $\partial J(\boldsymbol{\alpha}_n)/\partial\boldsymbol{\alpha}_n = \mathbf{0}$ yields the estimate $\boldsymbol{\beta}_n$ in (8) of the complex vector $\boldsymbol{\alpha}_n$ as given by

$$\boldsymbol{\beta}_n = (\mathbf{S}^H\mathbf{S})^{-1}\mathbf{S}^H\left(\mathbf{y}_n - \mathbf{s}_n\right). \tag{A3}$$

B. ESTIMATION WHEN INTERFERENCE AMPLITUDES ARE PURELY REAL

If the elements of the amplitude gain vector $\boldsymbol{\alpha}_n$ are real, that is $\boldsymbol{\alpha}_n = \boldsymbol{\alpha}_n^*$, we have from (A1)

$$\begin{aligned} J(\boldsymbol{\alpha}_n) &= \mathbf{y}_n^H\mathbf{y}_n - \mathbf{y}_n^H\mathbf{s}_n - \mathbf{y}_n^H\mathbf{S}\boldsymbol{\alpha}_n - \mathbf{s}_n^H\mathbf{y}_n + \mathbf{s}_n^H\mathbf{s}_n + \mathbf{s}_n^H\mathbf{S}\boldsymbol{\alpha}_n \\ &\quad -\boldsymbol{\alpha}_n^T\mathbf{S}^H\mathbf{y}_n + \boldsymbol{\alpha}_n^T\mathbf{S}^H\mathbf{s}_n + \boldsymbol{\alpha}_n^T\mathbf{S}^H\mathbf{S}\boldsymbol{\alpha}_n \end{aligned} \tag{B1}$$

Note that

$$\boldsymbol{\alpha}_n^T\mathbf{S}^H\mathbf{y}_n = \left(\boldsymbol{\alpha}_n^T\mathbf{S}^H\mathbf{y}_n\right)^T = \mathbf{y}_n^T\mathbf{S}^*\boldsymbol{\alpha}_n$$

$$\boldsymbol{\alpha}_n^T\mathbf{S}^H\mathbf{s}_n = \left(\boldsymbol{\alpha}_n^T\mathbf{S}^H\mathbf{s}_n\right)^T = \mathbf{s}_n^T\mathbf{S}^*\boldsymbol{\alpha}_n$$

since both quantities are scalars. Using the identity $\partial\mathbf{a}^T\boldsymbol{\theta}/\partial\boldsymbol{\theta} = \mathbf{a}$, we obtain the derivative of $J(\boldsymbol{\alpha}_n)$ with respect to the $(n-1)\times 1$ real vector $\boldsymbol{\alpha}_n$ as

$$\begin{aligned} \frac{\partial J(\boldsymbol{\alpha}_n)}{\partial\boldsymbol{\alpha}_n} &= -\mathbf{S}^T\mathbf{y}_n^* + \mathbf{S}^T\mathbf{s}_n^* - \mathbf{S}^H\mathbf{y}_n + \mathbf{S}^H\mathbf{s}_n + 2[\mathrm{Re}(\mathbf{S}^H\mathbf{S})]\boldsymbol{\alpha}_n \\ &= -\mathbf{S}^T(\mathbf{y}_n^* - \mathbf{s}_n^*) - \mathbf{S}^H(\mathbf{y}_n - \mathbf{s}_n) + 2[\mathrm{Re}(\mathbf{S}^H\mathbf{S})]\boldsymbol{\alpha}_n \\ &= -2\mathrm{Re}[\mathbf{S}^H(\mathbf{y}_n - \mathbf{s}_n)] + 2[\mathrm{Re}(\mathbf{S}^H\mathbf{S})]\boldsymbol{\alpha}_n \end{aligned} \tag{B2}$$

Setting $\partial J(\boldsymbol{\alpha}_n)/\partial\boldsymbol{\alpha}_n = \mathbf{0}$ yields the estimate $\boldsymbol{\beta}_n$ in (9) of the real vector $\boldsymbol{\alpha}_n$ as given by

$$\boldsymbol{\beta}_n = [\mathrm{Re}(\mathbf{S}^H\mathbf{S})]^{-1}Re[\mathbf{S}^H(\mathbf{y}_n - \mathbf{s}_n)]. \tag{B3}$$

REFERENCES

[1] W. Diffie, "Chattering about SIGINT," *IEEE Security Privacy*, vol. 4, no. 1, pp. 1–9, Feb. 2006.

[2] R. G. Wiley, *ELINT: The Interception and Analysis of Radar Signals*. Norwood, MA, USA: Artech House, 2006.

[3] *Joint Publication 1-02 Department of Defense Dictionary of Military and Associated Terms*, U.S. Department of Defense, Washington, DC, USA, Nov. 2010.

[4] J. V. Field, "Sigint and automation," *IEEE Ann. Hist. Comput.*, vol. 25, no. 1, pp. 65–69, Jan./Mar. 2003.

[5] P. E. Whittaker and M. S. Hodgart, "Small satellite SIGINT payload," in *Proc. IEEE Nat. Aerosp. Electron. Conf.*, Oct. 2000, pp. 625–632.

[6] J. F. Rivest and S. Rajan, "Morphological detectors for radar ELINT applications," in *Proc. IEEE Instrum. Meas. Technol. Conf.*, May 2013, pp. 1062–1067.

[7] W. Klembowski, T. Brenner, and W. Wizner, "Pit achievements in radar and elint technology," in *Proc. IRS Radar Symp.*, May 2006, pp. 1–9.

[8] B. Qing-long, Y. Jian, Z. Yue, and C. Zeng-ping, "LPI performance of digital array radars," in *Proc. IET Int. Radar Conf.*, Apr. 2009, pp. 1–4.

[9] S. M. Baarrij, F. Nasir, and S. Masood, "A robust hierarchical digital modulation classification technique: Using linear approximations," in *Proc. IEEE Int. Symp. Signal Process. Inf. Technol.*, Aug. 2006, pp. 545–550.

[10] K. N. Haq, A. Mansour, and S. Nordholm, "Recognition of digital modulated signals based on statistical parameters," in *Proc. 4th IEEE Int. Conf. Dig. Ecosyst. Technol.*, Apr. 2010, pp. 565–570.

[11] J. G. Andrews, "Interference cancellation for cellular systems: A contemporary overview," *IEEE Wireless Commun.*, vol. 12, no. 2, pp. 19–29, Apr. 2005.

[12] N. I. Miridakis and D. D. Vergados, "A survey on the successive interference cancellation performance for single-antenna and multiple-antenna OFDM systems," *IEEE Commun. Surveys Tuts.*, vol. 15, no. 1, pp. 312–335, Mar. 2013.

[13] R. A. Romero, T. T. Ha, and S. Lioulis, "Collection probability with discrete random signal-to-interference power ratios in multiple interferences for electronic intelligence receivers," *IET JoE*, DOI:10.1049/joe.2013.0035, pp. 1–8, 2013.

[14] S. Kay, *Fundamentals of Statistical Signal Processing*, vol. 1. Englewood Cliffs, NJ, USA: Prentice-Hall, 1993.

[15] H. Van Trees, *Optimum Array Processing*. New York, NY, USA: Wiley, 2002.

RIC A. ROMERO (S'07–M'10–SM'12) received the Ph.D. degree in electrical and computer engineering from the University of Arizona, Phoenix, AZ, USA, in 2010, the M.S.E.E. degree from the University of Southern California, Los Angeles, CA, USA, in 2004, and the B.S.E.E. degree from Purdue University, West Lafayette, IN, USA, in 1999.

He was a Senior Multidisciplined Engineer II with Raytheon Missile Systems, Tucson, AZ, USA, from 1999 to 2010. He was involved in various communications, radar, and research and development programs. He was also a Graduate Research Assistant with the Laboratory for Sensor and Array Processing, University of Arizona, from 2007 to 2010. He is currently an Assistant Professor with the Department of Electrical and Computer Engineering, Naval Postgraduate School, Monterey, CA, USA. His research interests are in the general areas of radar, sensor information processing, and communications.

Dr. Romero was awarded the 2004 Corporate Excellence in Technology Award, which is a company-wide technical prize at Raytheon Corporation. He was also granted the Raytheon Advanced Scholarship Program fellowships from 2002-04 and 2005-07.

ALEXANDER RIOS received the master's degree in electrical and computer engineering from the Naval Postgraduate School, Monterey, CA, USA, in 2013, and the B.S. degree from the United States Naval Academy, Annapolis, MD, USA, in 2007.

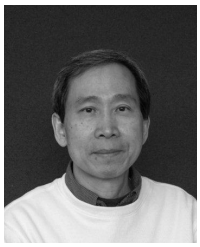

TRI T. HA has been a Professor with the Department of Electrical Engineering, Naval Postgraduate School (NPS), Monterey, CA, USA, since 1989. Prior to joining NPS, he was with Fairchild Industries, Lake Zurich, IL, USA, and General Telephone & Electronics Corporation, Stamford, CT, USA, and an Associate Professor with the Virginia Polytechnic Institute and State University, Blacksburg, VA, USA, for four years. He has authored three textbooks. His current research interests are in wireless communications and cyber warfare.